EUROPEAN COMMISSION

Community research

BELBaR

(Contract Number: 295487)

DELIVERABLE (D-N°:3.9)

Understanding of Radionuclide Colloid Interaction
(with special emphasis on sorption reversibility)

N. Sherriff and F. Livens; University of Manchester
N. Bryan; National Nuclear Labs
O. Elo, N. Huittinen and K Müller; Institute of Resource Ecology, Dresden, Germany
P Hölttä; Laboratory of Radiochemistry, University of Helsinki, Finland
U. Alonso and T. Missana; CIEMAT, Spain
F. Quinto, M. Lagos, M. Plaschke, T. Schafer, H. Geckeis; KIT, Germany
P. Steier; University of Vienna, Austria

Reporting period: **01/03/12 – 29/02/16**

Date of issue of this report: **08/07/15**

Start date of project: **01/03/12** Duration: 48 Months

Project co-funded by the European Commission under the Seventh Euratom Framework Programme for Nuclear Research &Training Activities (2007-2011)		
Dissemination Level		
PU	Public	

EURATOM

DISTRIBUTION LIST

Name	Number of copies	Comments
Christophe Davies (EC) BELBaR participants		

1 Introduction

This report describes the progress in the BELBaR project in the field of radionuclide bentonite colloid interactions. It starts with a summary of a review of the understanding of the reversibility of the interactions of radionuclides with bentonite (bulk and colloidal) before the start of the project. This has been included again in this third report, because an understanding of the previous literature is essential to understand the subsequent experiments.

This is the third report on this topic since the start of the BELBaR project. Therefore, the Introduction to this report contains a summary of the experiments that were reported in the previous report. Note: if preliminary data for an experiment were reported in the last report and the experiment has continued, then that work is reported in Section 3.

Section 3 contains a description of the current work of the BELBaR partners and anything not reported in the last report.

Important Caveat: For the data described here that have not yet been published in the open literature, the results reported here are **preliminary** and are subject to later reanalysis and reinterpretation. In particular, many of the BELBaR experiments are long-term studies to determine rate constants. In order that the current state of progress is clear, we have reported rate constants that have been calculated from the current data sets.

Following the description of the current state of work, there is a discussion of the current understanding of the reversibility of radionuclide-bentonite colloid interactions and the implications for radionuclide mobility in the vicinity of a high level radioactive waste repository with a bentonite backfill.

This work contains information on radionuclide-bentonite interactions only. There are of course other important processes that will affect the probability of bentonite colloid assisted transport, for example colloid stability, but these are discussed elsewhere.

2 Review of Current State of Knowledge

Before the start of experimental work in the BELBaR project, a thorough literature review was undertaken to determine the state-of-the-art. This section contains a summary of that review. It also includes in the relevant sub-sections, the completed experiments reported in last year's report.

2.1 The role of colloids in radionuclide transport

The importance of colloids in aiding the transportation of radionuclides depends on a number of factors. The type of bentonite and even the future climate, such as glacial melts altering the groundwater chemistry, could affect the importance of colloid mediated transport (Wold 2010). The various factors have been combined in the so called 'Colloid Ladder' (Mori et al 2003), which is shown schematically in Figure 2.1.

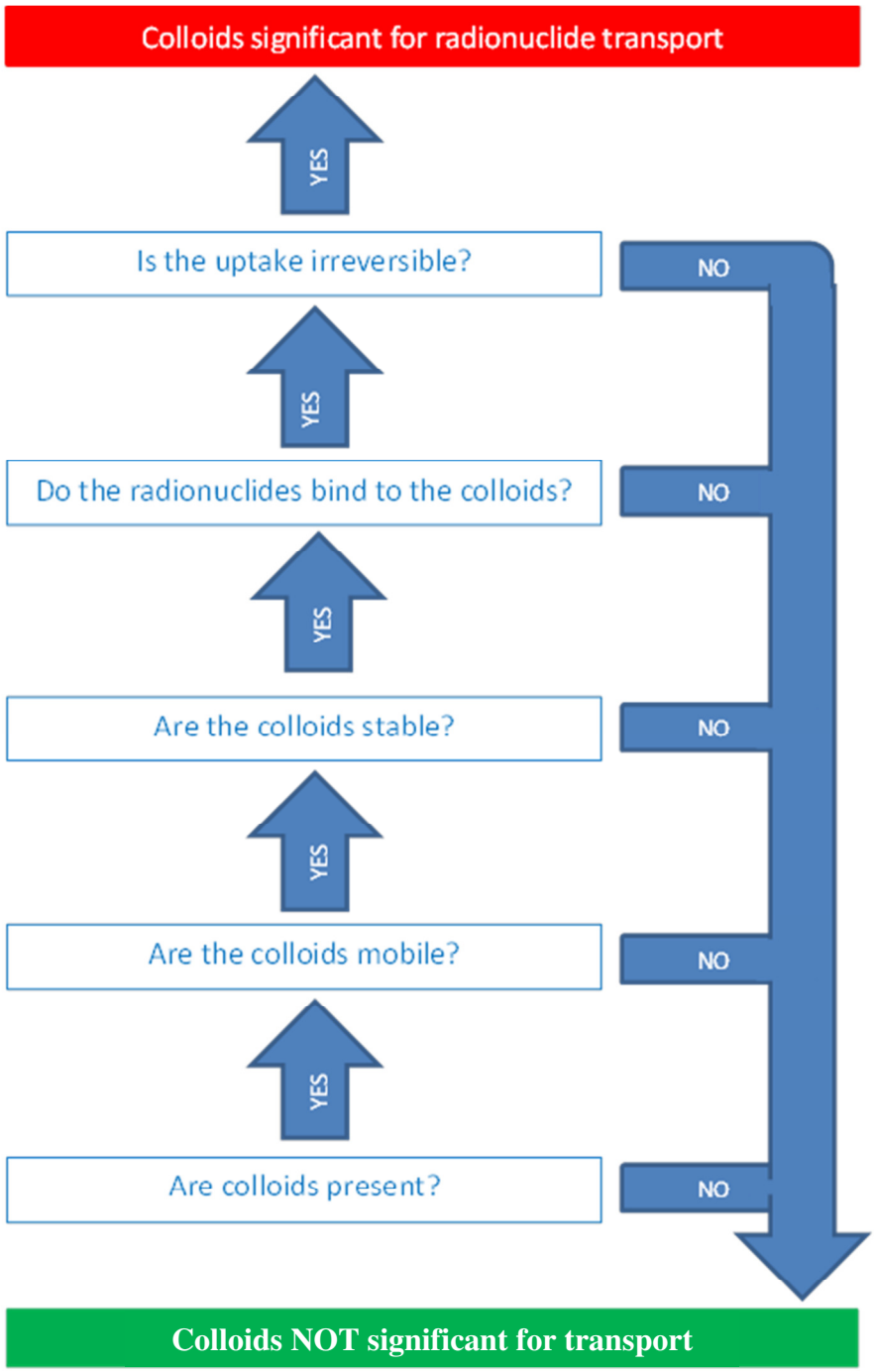

Figure 2.1. The colloid ladder (Mori et al 2003).

For colloidal transport to be significant, all of the following factors must be considered (Mori et al 2003; Missana et al 2008; Honeyman 1999; Miller et al 1994; Ryan and Elimelech 1996):

- **Are colloids present?** - If colloids are not present in the system, then they will not be able to promote radionuclide mobility, but if they are, then they may.
- **Are the colloids mobile?** – If the colloids themselves are not mobile, then they will not be able to promote radionuclide mobility.
- **Are the colloids stable?** - If the colloids are unstable, then any associated radionuclides would be removed from the mobile phase (the solution) as the colloids are destabilised.
- **Is there radionuclide uptake?** – If radionuclides do not bind to the colloids at all, then the colloids cannot promote transport.
- **Is uptake irreversible?** – If the binding of the radionuclide to the colloid is reversible, then colloids should not be significant for radionuclide transport, because the rock itself should be able to compete for binding of the radionuclide. If the binding were to be irreversible however, then transport of the radionuclide would essentially continue until the colloid stopped moving.

For colloids to be significant in the transport of radionuclides, then the answers to each of the questions listed above must be 'yes'. Here we will concentrate only on the last two of these.

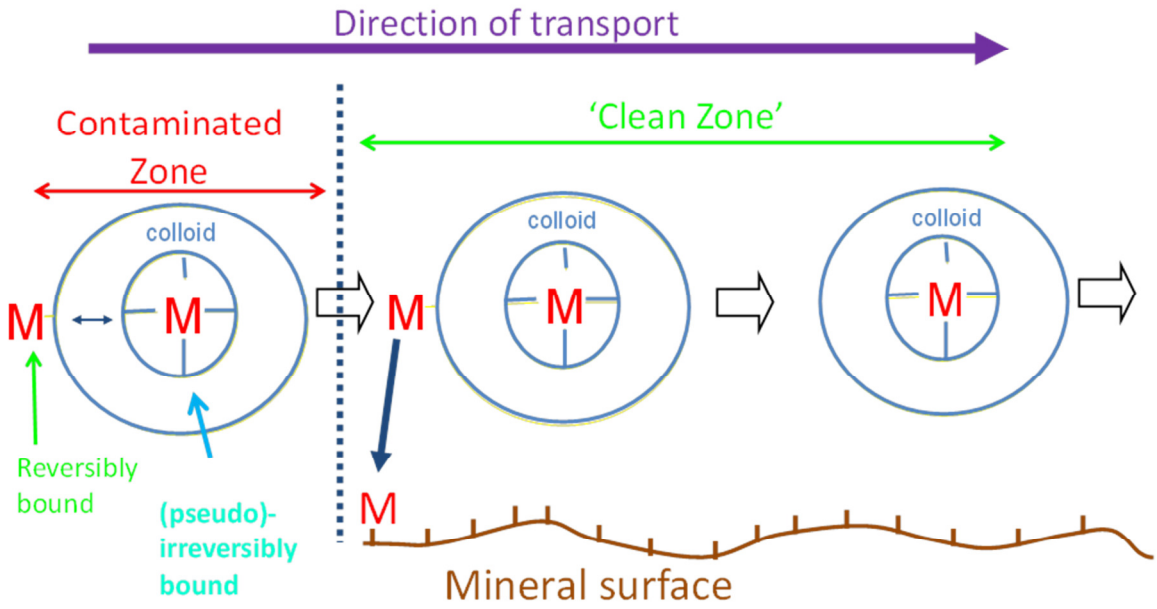

Figure 2.2: The mechanism for the transport of 'irreversibly' bound radionuclides (M).

Figure 2.2 shows the mechanism for the transport of irreversibly bound radionuclides. If colloids encounter radionuclides in a contaminated region, for example in or near a repository, then it is possible that they could become bound to the colloid, either reversibly or irreversibly. If the colloid then moves away, for example a bentonite colloid transporting through a fracture, then it would carry those bound radionuclides with it. However, it is expected that any radionuclides that are bound reversibly, and so may dissociate instantaneously, would be quickly and easily removed by the available rock surface binding sites that will be present in excess. In the case of irreversibly bound radionuclides, the strength of the competing sink will not remove the radionuclides, and the radionuclide will be transported with the colloids. In fact, the situation is more complex than this (Sherriff and Bryan 2013), because there is in fact no simple division between reversibly and irreversibly bound metal ions (see Section 2.4).

2.2 Radionuclide interactions with bulk bentonite

The interactions of radionuclides with bulk bentonite (and its constituents) have been studied extensively (Wold 2010). For example, Stumpf et al (2004) used TRLFS and EXAFS to study the coordination of trivalent actinide ions by the bulk. At ambient pH, they found that inner sphere complexes were formed with bonds to 4 oxygens on the surface, and approximately five waters retained. Rabung et al (2005) found a similar result for Eu(III) and Cm(III), with three different surface complexes, each with five waters/hydroxides in the coordination environment (as well as the surface oxygens): the number of hydroxides increases with pH. At very high pH (>12), Cm(III) forms a surface precipitate.

A number of models have been developed to explain and predict radionuclide surface complexation on bentonite (montmorillonite), e.g. Kowal et al (2004), but the two site protolysis non-electrostatic surface complexation and cation exchange (2SPNE SC/CE) model of Bradbury and Baeyens has proved particularly successful (e.g. Bradbury and Baeyens 1999; Bradbury et al 2005; Bradbury and Baeyens 2009; and refs therein). In this model, there are three inner sphere surface complexes for the trivalent actinides/lanthanides, $\equiv$SO-An^{2+}, $\equiv$SO-$An(OH)^{+}$ and $\equiv$SO-$An(OH)_2$, in addition to ion exchange sites. Unlike many surface complexation models, it is quasi-mechanistic: there is spectroscopic evidence for the predicted surface speciation (e.g., Rabung et al 2005) and there is a convincing correlation between the model equilibrium constants and radionuclide hydrolysis constants (Bradbury and Baeyens 2006).

Guo et al (2009) studied sorption and desorption of Eu(III) to bulk (Na)-bentonite, and found that for the bulk, the interaction was reversible over a period of a week. Only the irreversibility of Cs binding to bulk clays has been studied extensively (e.g., Comans, 1987; Comans et al., 1991; de Koning and Comans, 2004).

Work reported by Ivanov et al (Ivanov et al 2013), reported on the reversibility of the interactions of ^{237}U and ^{237}Pu at very low concentrations (8.4×10^{-11} M and 3.7×10^{-11} M, respectively), close to the actinide concentrations expected in the environment. Humic acid (HA) was used as a competing ligand in a study of the intaction of ^{237}U(VI) and ^{237}Pu(III) with bentonite. In the presence of humic acid, the uranyl uptake by bentonite was significantly modified. The sorption of humic acid on bentonite was also studied and the general trend is of decreasing uptake with increasing pH, and at pH higher than 7.8 (pHpzc of bentonite), the uptake is negligible. The retention of U(VI) in the presence of humic acid was more complex. At low pH, the addition of HA enhances U(VI) sorption which indicates ternary surface complex formation. In the range between pH 3.8 and 6.5, the sorption of U(VI) is reduced in by the presence of humics. At pH between 7 and 9, the uranyl uptake is slightly enhanced in the presence of HA. At very high pH, the uranium sorption is less sensitive to the presence of humic.

The effect of the addition order of the ternary system components in the ^{237}U(VI) and ^{237}Pu(III)/bentonite/humic acid ternary systems was investigated, and an example of the results is given in Figure 2.3. The kinetics of uranyl distribution between the supernatant and the solid phase was found to be relatively slow and approximately four days were required to reach equilibrium in the presence of HA. In the absence of HA, the system reaches apparent equilibrium more quickly (although 1 day is still required for maximum sorption). The most significant result was that there was no evidence for irreversibility, or even slow dissociation for uranyl.

The results for ^{237}Pu(III) were very different. This time, the dissociation of the Pu from the bentonite was slow, and even after 25 days, the system had not reached equilibrium. Note, although there was evidence of slow dissociation, there was no direct evidence for irreversibility.

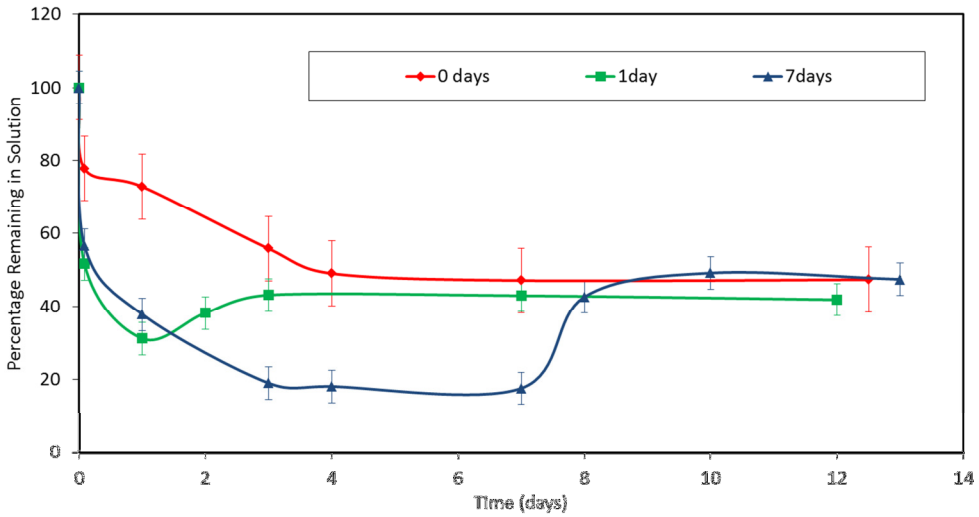

Figure 2.3: Effect of addition order in the U(VI)-bentonite-humic acid ternary system.

Sherriff et al (2013) reported some experiments to study the behaviour of Eu in bentonite/Eu(III)/HA ternary systems, again at low concentrations (7.91 x 10^{-10} M): the data are shown in Figure 2.4. Significantly, there was evidence for slow uptake, even in the absence of humic acid. For a simple Eu(III)/bentonite binary system, it takes 14 days before an apparent steady state concentration of Eu is remaining in solution. The increase in the amount of Eu bound is approximately 2.5% in this HA-free system between 1 and 14 days. This seems small, but it corresponds to an increase in K_d by a factor of approximately 4 (decrease in percentage Eu free in solution from 3.6 % to 0.97 %), and so there is an increase in effective binding strength. Therefore, some mechanism must be taking place that allows this. It seems highly unlikely that this can be explained by simple surface complexation (even multiple sites), because this would be expected to take place much quicker for a lanthanide (III) ion.

A mathematical model was developed to describe the uptake of humic acid and Eu(III). The fits to the experiments are given as the lines in Figure 2.4. The model performance and equations were discussed previously (Sherriff et al 2013).

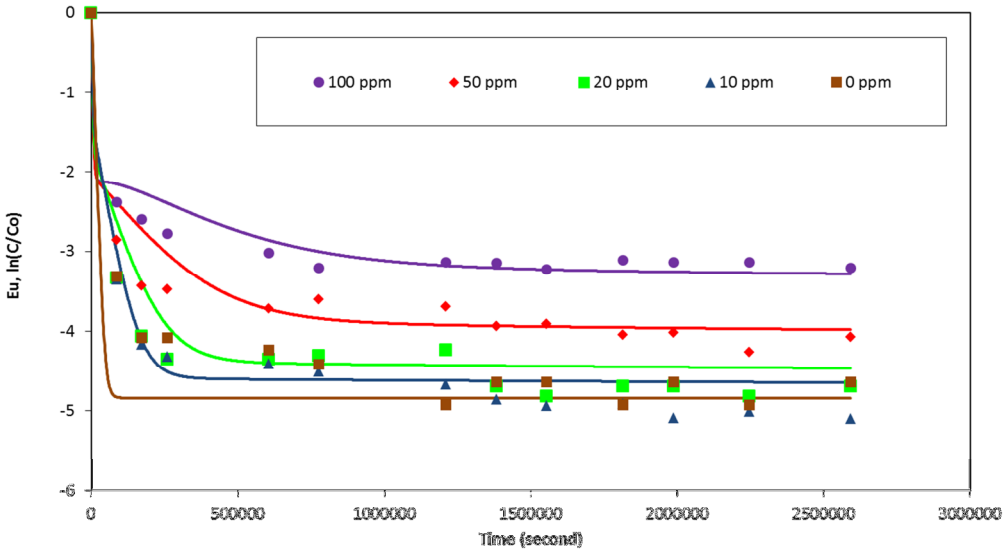

Figure 2.4: Model fit to Eu kinetic uptake data as a function of humic acid concentration.

2.3 Radionuclides and colloidal bentonite and reversibility

Theoretical calculations by NAGRA (NAGRA, 1994) have shown that 'irreversibility' associated with colloidal ternary systems may significantly influence radionuclide mobility from a repository. Further, inorganic colloids have been implicated in the enhanced migration of radionuclides in the environment (Kersting et al 1999). It has been found that under the correct conditions, bentonite colloid associated radionuclides can travel faster than a conservative tracer (Geckeis et al 2004). Calculations have shown that the slow dissociation of radionuclides from solution phase colloids (short of 'irreversibility') can result in the rapid transport of radionuclides: in order to have an effect, the residence time of the colloidal material in the solution only needs to be less than the half time of the dissociation reaction, migration increasing with reaction half-time (Bryan et al 2007). The effect of slow dissociation kinetics (and colloid sorption) may be assessed using an approach based on Damkohler numbers (Bryan et al 2007).

Although radionuclide uptake onto bulk bentonite and montmorillonite have been studied extensively, sorption to bentonite colloids has not, and the critical dissociation kinetics barely at all (Wold 2010). Geckeis et al (2004) determined K_d values for uptake onto bentonite colloids of 1.2×10^6–2.7×10^6 l kg^{-1} for Am(III) and 1.0×10^5– 8.0×10^5 l kg^{-1} for Pu(IV). The values for Cs(I) and U(VI) are significantly lower, 6.4×10^3–8.7×10^3 l kg^{-1} and 0.8×10^3–2.5×10^3 l kg^{-1}, respectively. The data for Am(III) are in the range for bulk montmorillonite, suggesting that the sorption mechanisms are similar, but Mori et al (2003) suggest that the values for Am(III) and Pu(IV) are slightly higher than for bulk bentonite, which they attribute to the larger specific surface area. Further, although the sorption strength seems constant with time for Am(III), Mori et al (2003) report an increase of an order of magnitude over the course of 3 weeks for Pu(IV). Interestingly, the TRLFS spectrum of Cm(III) bound to (FEBEX) bentonite colloids, suggests a surface complex of the form $\equiv SO{-}Cm(H_2O)_{5-x}(OH)_x$ ($x \leq 5$), which is similar to that of Cm sorbed to bulk montmorillonite (see above; Geckeis et al 2004). There was also evidence for complexation by organic material naturally present in the bentonite (Geckeis et al 2004). For Am(III) and Pu(IV), the strong interaction with bentonite colloidal material is sufficient to reduce the apparent K_d for sorption to the bulk rock by an order of magnitude. Missana et al (2008) have also measured K_d values for Eu(III), $5.6x10^5$ - $8.1x10^5$ l kg^{-1}, and Pu(IV), $1.5x10^5$ - $3.5x10^5$ l kg^{-1}. Wold (2010) collated experimental colloid K_d values: for Am(III) values lie in the range 10^4 - $2x10^8$ l/kg , whilst those for Pu(IV) range between 1 - $2.3x10^5$ l kg^{-1}, and for U(VI) the range is $8.1x10^2$ - $1.6x10^3$ l kg^{-1}.
However, Ijima et al. (2008) performed sorption experiments with Am and bentonite colloids at pH 8 and 10. Even before the addition of bentonite colloids, they found that Am radiocolloids were formed. Iijima et al. (2010) performed batch experiments with Cs and Am with granite and bentonite colloids in an N_2 atmosphere at pH 9.6. They prepared 3 batches, with different orders of addition using bentonite colloids (C), granite (G) and the radionuclide (R). Batch 1 was CR+G (i.e. bentonite colloids and radionuclide were initially equilibrated, then granite was added after 100 days), batch 2 was GR + C and batch 3 was GC + R. They found the binding of Am to bentonite colloids to be fully reversible, but also demonstrated the formation of Am radiocolloids for both the CR + G and GC + R batches. They cautioned that the formation of Am radiocolloids could lead to over estimations of the amount of Am bound to bentonite colloids.

Although models based on instantaneous equilibrium have been proposed for the prediction of radionuclide movement through bulk bentonite (e.g. Ochs et al 2003), kinetic processes are thought to be significant for bentonite colloid mediated transport. Experiments with actinides and technetium with bentonite colloids in the presence of fracture filling material showed 2 distinct types of behaviour: U(VI), Np(V) and Tc(VII) did not associate with the bentonite derived colloids, but Th(IV), Pu(IV) and Am(III) did (Bouby et al 2010A**;** Huber et al 2011). When the colloids were contacted with fracture fill material, dissociation was observed, which started after 100 - 300 hrs of contact and continued over 1000s of hours. There was some evidence that the system was approaching equilibrium after approx. 7,500 hours (Bouby et al 2010A**;** Huber et al 2011). Huber et al (2011) have provided dissociation rate constants for these experiments. For Am(III), the values were in the range 0.0037 - 0.009 hr^{-1} (1 - 2.5 $x10^{-6}$ s^{-1}), whilst for Pu(IV), the range is 0.0014

- 0.0085 hr^{-1} (3.9 $x10^{-7}$ - 2.4 $x10^{-6}$ s^{-1}). The apparent initiation period for dissociation contrasts with the behaviour for naturally occurring organic colloids, where a range of dissociation constants are observed, and dissociation commences immediately upon contact with a stronger sink (King et al 2001; Monsallier et al 2003). Wold (2010) has also estimated representative first order dissociation rate constants (k_b) for: Pu(IV) $4.35x10^{-3}$ hr^{-1} (= $1.2x10^{-6}$ s^{-1}); Am(III) $2x10^{-3}$ hr^{-1} (= $5.6x10^{-7}$ s^{-1}); Np(IV) $4.6x10^{-7}$ hr^{-1} (= $1.2x10^{-10}$ s^{-1}); Cm(III) $6x10^{-3}$ hr^{-1} (= $1.7x10^{-6}$ s^{-1}); U(VI) $3x10^{-3}$ hr^{-1} (= $8.3x10^{-7}$ s^{-1}); Tc(IV) 0.63 - 15 hr^{-1} (= $1.75x10^{-4}$ - $4.2x10^{-3}$ s^{-1}). However, these values were estimated from sorption rate constants (k_f) and assuming that $K_d = k_f/k_b$, and so they must be treated with care.

Bouby et al (2010B) found that for Eu(III), Tb(III) and Th(IV) ions, the colloid associated fraction was in the range 95 – 100 %, which was in agreement with the work of Missana et al (Missana et al 2008), which showed > 75% colloid bound for Eu(III) and Pu(IV). Schäfer et al. (2004) found that approximately 80% of Th(IV) and Eu(III) were colloid associated. Despite the apparent similarity in their amounts associated with colloids, transport experiments through a Grimsel rock core found that Th(IV) was more permanently associated with the clay colloids during transport than Am(III) and Tb(III). In fact, in a series of experiments, the Th(IV) was found to elute with the colloids. Bouby et al (2010B) suggest that there is a relationship between residence time and An(IV) (and colloid) recovery by comparison of their data with the data of: Hauser et al. (2002); Möri et al. (2003); Geckeis et al. (2004); Missana et al. (2003); Schäfer et al. (2004); Missana et al. (2008). Although there did seem to be slow dissociation, there was no evidence for irreversible binding of radionuclides, and over a period of the order of a year, equilibrium partition between colloid and fracture fill seemed to be established. Bouby et al (2010C) found that there appeared to be a discrepancy between the rates from batch and column experiments, with dissociation rates higher in transport experiments than in batch, but the reason was unclear. Transport calculations on the field scale for flow through fractures suggested that, provided the dissociation rate is greater than 0.2 yr^{-1} ($6.34x10^{-9}$ s^{-1}), then the kinetics do not have a significant effect on radionuclide mobility, although the limit will actually depend upon the distance of interest and the flow rate (see Section 4). The authors suggested that future research should concentrate on processes that could result in such very slow dissociation (e.g. coprecipitation).

Geckeis et al (2004) found that Am(III) and Pu(IV) transport through fractures could only be explained by slow dissociation from colloids, although the interactions were eventually reversible on a time scale of months. The mechanism for slow dissociation was unclear: slow diffusion from pores could be responsible for slow Cs/Sr(II) dissociation, but it was suggested that slow break-up of surface complexes was a possible explanation for f-block ions. In lab (core) column experiments, Missana et al. (2008) found that Eu(III) transported associated to colloids, but dissociation did take place during transport. Taking into account the residence time of the colloid associated Eu, the percentage recovery of the colloids and the amount of Eu that was associated with the colloids, it is possible to estimate an overall first order dissociation rate constant (4.8×10^{-4} s^{-1}). This is higher than rates from batch experiments (see above), but it does match with the discrepancy between column experiment and batch rates observed by Bouby et al (2010C). For Pu(IV), the recovery could be predicted directly by the colloid recovery, which could suggest that the dissociation of Pu(IV) may be slower. Given that no dissociation was observed in the column experiment, it is not possible to calculate a dissociation rate for Pu(IV), but it is possible to estimate an upper limit. Given the residence time in the column, if the minimum Pu dissociation that could be observed were 10%, then the rate constant must be less than 10^{-5} s^{-1}. The data of Missana et al (2008) show the importance of dissociation kinetics, since the same authors measured a slightly higher K_d for Eu(III) onto the colloids (ΔlogKd = 0.46). Iijima et al (2010) observed slow dissociation of bentonite colloid associated Am in a granite ternary system, but no evidence for 'irreversibility'. Interestingly, they too found that the bulk rock K_d was reduced by approximately an order of magnitude when granite was added to Am pre-equilibrated with the colloids. Delos et al (2008) studied the transport of bentonite colloids through a ceramic column. They showed that larger colloids eluted first. Am(III) and Pu(IV) elution was closely related to that

of the colloids, although the Am and Pu recovery was less than that of the colloids themselves, which was interpreted as evidence of dissociation during the experiment.

Bouby et al (2011) found that Cs(I) and U(VI) did not bind to bentonite colloids, but once again the tri- and tetravalent f-block ions (Eu(III); Th(IV)) were strongly associated with the colloids. The Th(IV) was preferentially associated with the smaller colloids, which was attributed to their larger specific surface area. They also studied the competition between bentonite colloids and humic acid. In the case of Eu(III), they found that although dissociation from the inorganic colloids was slow, equilibrium was eventually obtained, and most of the Eu(III) dissociated from the bentonite colloids and bound to the humic. Most importantly, the eventual distribution was the same as that in experiments where the Eu was not pre-equilibrated with the bentonite colloids. However, in the case of Th(IV), even after 3 years, the amount of Th bound to the bentonite colloids was greater than that in a system where Th(IV) had not been pre-equilibrated with them. Therefore, for this ion at least, there does seem to be some 'irreversibility' on a time scale of 3 years. The reasons for this irreversibility are unclear, but the authors suggest that it might be due to the formation of a surface precipitate. Interestingly, Morton et al (2001) used XAS to study Cu surface coordination to bulk montmorillonite. They found that under the conditions where 'irreversibility' was observed, Cu - Cu interactions were observed. The authors interpreted the data in terms of the sorption of Cu dimers.

Wold (2010) has suggested than radionuclide ions attached to colloids via an ion exchange mechanism are unlikely to transport, because dissociation is instantaneous, and the far-field rock surface area is much larger. It is more likely that radionuclides sorbed by inner sphere surface complexation will show slow dissociation kinetics and so will be transported. That said, although slow dissociation would be possible for inner sphere surface complexes, 'irreversibility' would not be expected (Schäfer (2012).

Beyond bentonite colloids that are produced by erosion of the clay, there is the possibility of colloid formation where the bentonite pore water mixes with the background groundwater (Kunze et al 2008). Kunze et al (2008) studied the mixing of bentonite (FEBEX) pore water and Grimsel groundwater. They showed that Th(IV), Eu(III) and Cm(III) could be significantly colloid associated in the mixing zone. This result is significant, because as well as providing 'new' colloids that could act as a transport vector for radionuclides, there is the possibility that radionuclides could be incorporated as they form. Incorporation is more likely to result in very slow (pseudo irreversible) dissociation than simple surface complexation.

Missana et al (2013) reported some transport experiments in a Grimsel granite fracture using a water flow velocity from $1 \cdot 10^{-6}$ to $1 \cdot 10^{-5}$ m/s (corresponding to a residence time between 2 and 20 hours), injecting cesium ([Cs]=$1 \cdot 10^{-7}$ M) or 100 ppm of bentonite colloids on which Cs was previously adsorbed. In those systems, > 80 % of the cesium was absorbed onto the bentonite colloids prior to their injection. The results of the experiment are shown in Figure 2.5.

The breakthrough curve of cesium, without colloids, presented a single peak with a retardation factor (Rf) of ~200. In the presence of bentonite colloids, the breakthrough curve clearly showed a small cesium peak in a position very similar to that of the conservative tracer (HTO), with an Rf of 0.8, which was interpreted as colloid associated Cs. It is quite clear that the first peak of Cs, seen in the breakthrough curve, is coincident with the colloid breakthrough peak. However, the quantity of cesium recovered after this peak was only the 0.15 % of the injected, although the colloid recovery was quite high (80%), and completed after less than 10 pore volumes. Since only 0.15% of the injected cesium was recovered at this stage, this result suggests that the cesium had desorbed from colloid, presumably because of competition from sorption sites on the solid.

In summary, slow dissociation kinetics can enhance the transport of radionuclides. Further, although for some species (e.g. uranyl and cesium) there is some evidence that dissociation is

fast, there is some evidence of very slow dissociation of trivalent and tetravalent ions under certain conditions, which could have significant consequences for actinide transport. Unfortunately, the mechanisms are not understood, and currently reliable predictions of radionuclide mobility are not possible.

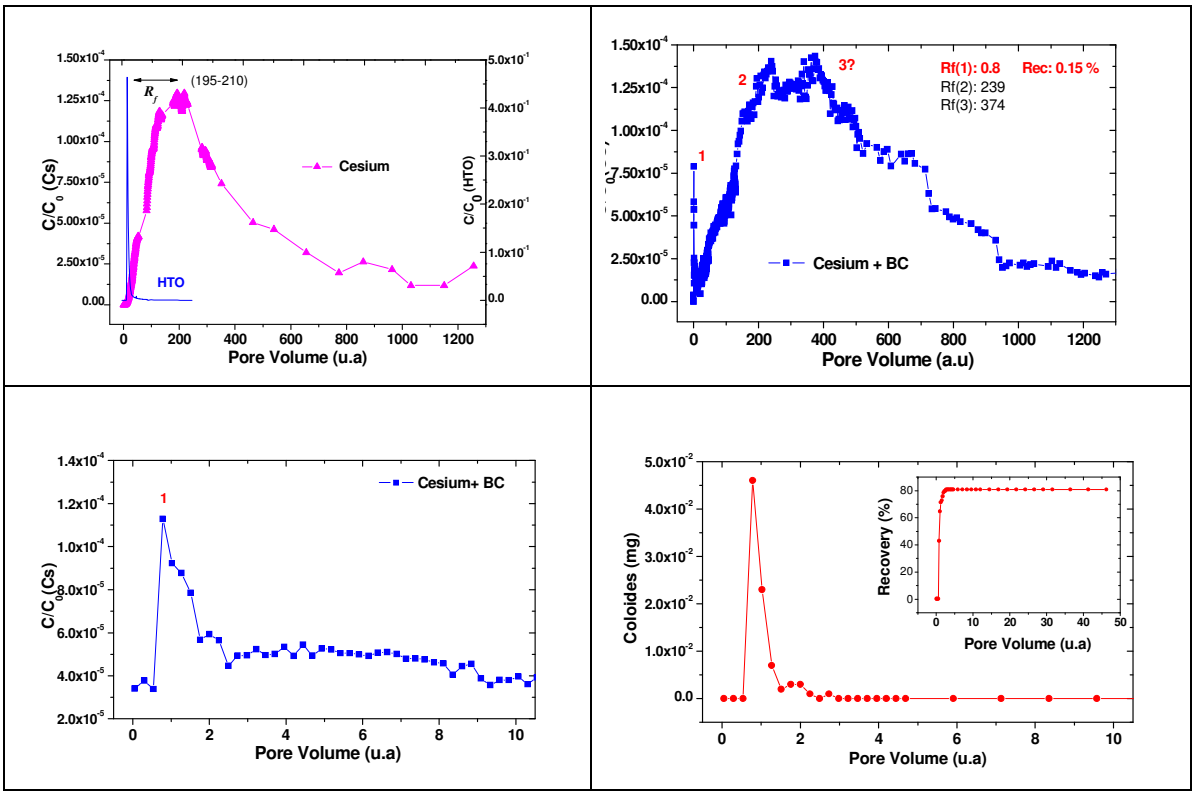

Figure 2.5: Breakthrough curve of cesium: top left, without bentonite colloids; top right, in the presence of 100 ppm bentonite colloids. Initial stages of the breakthrough curve of cesium: bottom left, Cs activity measurements; bottom right, PCS measurements (in the inset the recovery of colloids is shown).

2.4 Colloid kinetics in the safety case

The test for radionuclide-colloid interactions in the Colloid Ladder (see above) is whether the interaction is 'irreversible'. However, the situation is more complex than such a simple 'yes or no' question. First, no radionuclide sorption and/or incorporation process will truly be irreversible, and given sufficient time any bentonite colloid associated radionuclide will eventually be able to leave the colloid, although that could take a very long time. The important question is whether the time that would be taken for the radionuclide to be released from the colloid is greater or less than the timescale of interest.

Sherriff and Bryan (2013) reported a methodology for assessing the importance of colloid dissociation kinetics in transport calculations, based on the use of Damkohler numbers (Jennings and Kirkner 1984).

The dimensionless Damkohler number for a metal ion (radionuclide) in the slowly dissociating fraction, D_M, is defined by,

$$D_M = \frac{L}{V} k_b$$

where, L is the length of the column, and V is the linear flow rate. The behaviour is controlled by the value of the dissociation rate constant, k_b, and systems with the same values of D_M will show the same behaviour. As k_b (and so D_M) varies, there are two limiting behaviours. At high values of

k_b, dissociation kinetics will be unimportant, and a simple equilibrium (K_d) approach can be used to describe the interaction of the radionuclide with the colloids. At lower k_b, kinetics will dominate the behaviour, and provided that the colloid itself is not retarded, the behaviour of the radionuclide will tend towards that of a conservative tracer.
The kinetics of colloid association with the mineral surface affect the transport behaviour of the radionuclide. We can define a Damkohler number for the colloid removal process, D_C,

$$D_C = \frac{k_a}{V} L$$

If a colloid with an associated radionuclide is removed from solution, then that in itself will cause some retardation. However, it will also increase the residence time of the complex in the water column, allowing more time for dissociation of the radionuclide and immobilisation on the rock surface. The extent of this effect will depend upon the affinity of the colloid for the surface and the colloid Damkohler number (D_C). If D_C is small, then the residence time is too short for removal from solution to be significant, the complex transports with the velocity of the groundwater, and there is no effect upon the metal-humic kinetics, i.e. the behaviour of the metal is still controlled solely by k_b, and D_M may still be used to define the behaviour of the contaminant,

$$D_M = \left. \frac{k_b}{V} L \right|_{D_C \to 0}$$

However, in the case of significant retardation of the colloid, the Damkohler number for the slowly dissociating radionuclide must be adapted to take account of the increased residence time. If D_C is large ($D_C \rightarrow \infty$), and the humic sorption process may be described with an equilibrium constant, K_C, then the effective metal ion Damkohler number, D_M^{eff}, will be given by,

$$D_M^{eff} = \left. \frac{k_b}{V} L (1 + K_C) \right|_{D_C \to \infty}$$

Where K_C is the equilibrium distribution coefficient for the colloid between the solid and solution phases. For systems with intermediate values of D_C, these equations may be used to provide a range of Damkohler numbers, the most representative value lying somewhere in between.

To assess the importance of slow dissociation kinetics in a system that includes colloid immobilisation processes and to determine the most appropriate approximations, first one should calculate D_C. If it is small, then D_M may be used to determine whether slow dissociation kinetics are significant, whilst if it is large, D_M^{eff} should be used. If D_C has an intermediate value, then D_M will provide an indication of the maximum possible effect of slow dissociation, and D_M^{eff} the minimum. Figure 2.6 shows the procedure that should be used for selecting the most appropriate approximations if any, to describe slow dissociation and colloid removal processes. The flow sheet in the figure provides the most appropriate approximations (if any) for systems including colloid immobilisation and slowly dissociating radionuclides. MAX1 and MIN1 are the arbitrary Damkohler number limits for the colloid removal, and MAX2 and MIN2 are the limits for the slow dissociation of radionuclides from colloids. These values would depend upon the requirements of the calculation and the acceptable errors.

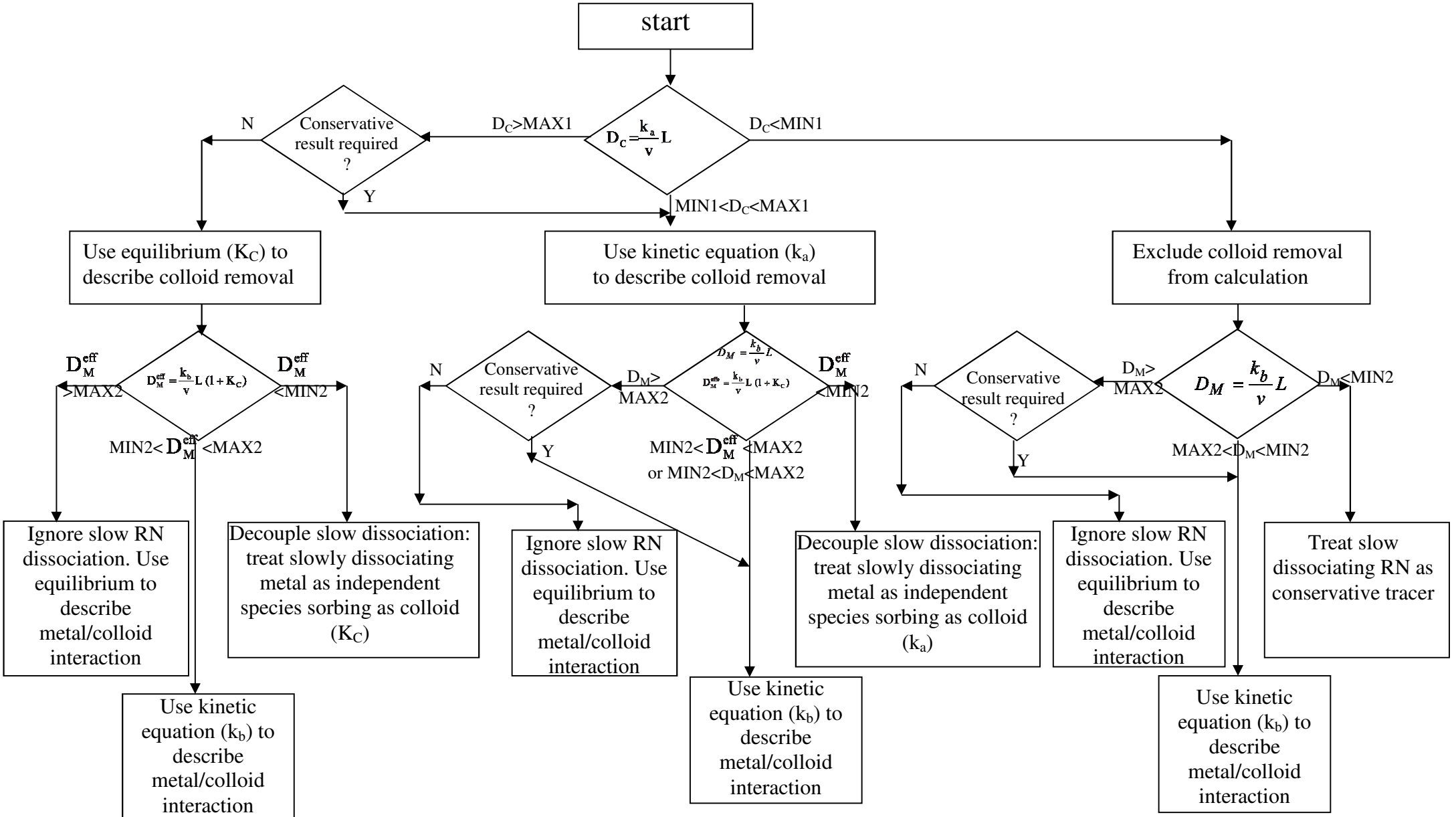

Figure 2.6: Colloid kinetics flowsheet.

3 Experimental Data From BELBaR Partners

This section describes the experimental data from the BELBaR partners that have been produced in the last 12 months, since the previous report.

A running theme through all of this experimental work is the concept of competition. The study of the uptake by bentonite is relativey straightforward, and requires only that the radionuclide is introduced to the clay. However, to study the reversibility of the interaction, it has been necessary to allow the radionuclide to interact with the bentonite before using a competiting ligand or cation binding resin or other strong radionuclide sorber as a strong sink to 'pull' the radionuclide from the bentonite, so that the dissociation rate may be measured.

There is direct spectroscopic evidence that the interaction of radionuclides with bentonite colloids is the same as that with bulk material. It is easier to study radionuclide binding by bulk material than colloidal, because of the straightforward phase separation. Hence, some of the work in BELBaR has focussed on the reversibility of radionuclide sorption to bulk bentonite, because surface complexation and incorporation effects would be expected to be similar.

3.1 Eu/Bentonite ternary systems

The authors involved in the work in this section are: N. Sherriff, F, Livens (*Centre for Radiochemistry Research, School of Chemistry, University of Manchester, Manchester, U.K.*) and N.D. Bryan (National Nuclear Laboratory, 5th Floor, Chadwick House, Birchwood, Warrington, WA3 6AE, UK).

In these experiments, the interaction of europium with bentonite has been studied.

3.1.1 Materials and Methods

The clay used in this work is a sodium Wyoming bentonite. All water was deionised (18 MΩ) and all reagents were analytical grade. All experiments were repeated in triplicate.

Preliminary Eu dissociation experiments

Preliminary experiments had to be performed to establish what quantities of materials would be used for the batch dissociation experiments. Preliminary sorption experiments were performed with ^{152}Eu (1 ml, 1 kBq), deionised water (8 ml) and $NaClO_4$ (1 ml, 0.1 M), to this was added bentonite clay (0.05 g, 0.1 g and 0.5 g). The samples were adjusted to pH 7 ($\pm$ 0.1). They were left on a slow rocker for 68 hrs before centrifugation (10 ml, 4000 rpm, 15 mins followed by 2 ml, 14000 rpm 35 mins) and analysis on the gamma ray detector to determine the amount of bentonite clay required to remove nearly 100% of the ^{152}Eu from the solution.

Preliminary dissociation experiments were then performed using ^{152}Eu (1 ml, 1 kBq), deionised water (8 ml) and $NaClO_4$ (1 ml, 0.1 M). EDTA was added (0.1 M, 0.01 M, $1x10^{-3}$ M and $1x10^{-4}$ M) and the pH adjusted to 7 ($\pm$ 0.1). Following addition of EDTA, bentonite (0.5 g) was added. The samples were left on a slow rocker for 18 hrs. Centrifugation (10 ml, 4000 rpm, 15 mins followed by 2 ml, 14000 rpm 35 mins) was performed and the solution was analysed by gamma ray spectrometry to determine the amount of EDTA required to retain nearly 100% of ^{152}Eu from the bentonite.

Bulk Eu dissociation experiments

Bentonite clay (0.5 g) was added to tubes with deionised water (8 ml), $NaClO_4$ (1 ml, 0.1 M) and ^{152}Eu (1 ml, 1 kBq) to give a total Eu concentration of 7.9×10^{-10} M, the system was then adjusted to pH 7 ($\pm$ 0.1). The clay was suspended (maximising contact with the Eu(III)) and the tubes were left on their sides, maximising contact between dissolved species and the clay. After a pre-equilibration period between 1 and 332 days, EDTA sodium salt was added to the system. Before the addition of EDTA, the tubes were centrifuged on a BOECO C-28A centrifuge (15 mins, 4000 rpm) to remove particles larger than 2 µm. Once this was complete, the top 4 ml of suspension in the tube were removed and distributed into 2 ml containers. These were then centrifuged (35 minutes, 14000 rpm): this removed all particles larger than 0.25 µm. Following centrifugation, 1 ml of the solution was removed and replaced by EDTA, which when introduced to the 10 ml system gave an EDTA concentration of 0.01 M. Once the EDTA was added, the tubes were rocked for 1 hour to re-suspend the clay. Following the re-suspension, and after a period of 1 day, the tubes were again centrifuged as before, and 1.5 ml were removed for analysis by gamma ray spectrometry (Canberra 2020 coaxial HPGe gamma spectrometer with an Ortec 919E multi-channel analyser). The aliquots were then returned to the sample tube, the clay re-suspended and the sample stored for later analysis. In a separate experiment, the uptake of Eu on to bentonite was measured in the absence of EDTA, but under the same conditions. Also, an experiment was performed where EDTA was added to the Eu tracer solution, prior to any contact with the bentonite clay (this was to ensure that the EDTA could effectively compete with the clay for the Eu).

Colloid studies

Colloid Formation

The experimental techniques have been adapted from Bouby et al (2011). The clay was sieved to <63 µm. 10 g of bentonite clay was soaked in 1 L deionised water for 10 days, and the beaker was covered in protective foil to ensure no contamination and also to ensure no loss of water through evaporation. To aid the generation of colloids, through abrasion, the suspension was kept stirring through the entire 10 days. The resulting bentonite slurry was evenly distributed into centrifuge tubes (50 ml x 20), even slurry distribution was achieved by keeping the slurry stirring and extracting the required 50 ml using a syringe. Each tube was centrifuged (4000 rpm, 11 minutes); this was calculated to ensure no bentonite colloids remaining in solution were larger than 500 nm. Each tube had the supernatant fluid decanted, and was then refilled to the 50 ml mark with deionised water and sonicated in a sonic bath for 10 minutes to re-suspend the clay. This process of centrifugation and sonication was repeated a further 3 times. The supernatant fluid remaining after the 4^{th} centrifugation step constituted the colloidal stock, which was stored in the dark.

Concentration determination

ICP-AES (Inductively coupled plasma atomic emission spectroscopy) was used to measure the concentration of the colloids. Each sample was diluted with deionised water (1 ml sample, 9 ml deionised water), and to this HNO_3 was added (0.2 ml) prior to analysis to determine the concentrations of Al and Mg (method adapted from Laaksoharju, 2005).

Size distributions

Syringe filters and ultrafiltration membranes were used sequentially to filter the bentonite colloid stock (450, 200 and 100 nm PES filters). The filters and membranes were adjusted to the pH of the colloid suspension (8.8 ± 0.2) and pre-equilibrated for 68 hrs prior to use. Ultrafiltration was performed under pressure (argon, 1.5 bar) through membranes (Millipore, polyethersulfone: 300, 10 and 3 kDa). In a separate experiment, ^{152}Eu (3.5 ml, 35 kBq) was added to a sample of the bentonite colloid stock (3.5 ml) and left for 68 hrs to equilibrate before filtration as above. The syringe filters and ultrafiltration membranes were pre-treated in 10^{-4} M stable $Eu(NO_3)_3$ solution to prevent sorption of the radiotracer, according to the method of Pitois et al. (2008).

Dowex preparation

Dowex ion exchange resin was used as a competitor for the colloid experiments. The Dowex used in these studies was Dowex resin 50WX4-200. The resin was supplied in hydrogen form. For use as an efficient ion-exchange competitor for Eu(III) (that will not change solution pH), it was converted to its sodium form. 20 g of Dowex resin were added to a sintered column, and washed with: deionised water (150 ml); HCl (2 M, 500 ml); deionised water (500 ml); NaCl (3 M, 500 ml); NaOH (0.1 M, 500 ml); and finally deionised water (500 ml). The washed resin was then spread onto a watch glass and was allowed to dry, before being stored ready for use in a plastic pot that was sealed (Li, 2011).

Europium/colloid dissociation batch experiments

Preliminary experiments were performed to establish what quantities of materials would be used for the colloid batch experiments. Preliminary sorption experiments were performed with ^{152}Eu (1 ml, 1 kBq) and deionised water (9 ml). To this mixture, various quantities (0.2 – 1.4 g) of Dowex resin were added, and the pH was adjusted to the pH of the colloid suspension (8.8 ± 0.2). The systems were left to associate on a slow rocker for 18 hours. After association, the samples were centrifuged (10 ml, 4000 rpm) and the supernatants were analysed on the gamma ray detector to determine the amount of dowex required to remove nearly 100% of the ^{152}Eu from the solution.

Once the ^{152}Eu was bound to the resin, the supernatant was removed and replaced with an equal volume of colloid suspension to investigate the dissociation from the resin to the colloids. These samples were allowed to rock for 18 hrs before centrifugation (10 ml, 4000 rpm) and analysis of the supernatant for ^{152}Eu content.

^{152}Eu (30 ml, 30 kBq) was added to a container, where its pH was adjusted to match the pH of the colloid suspension (8.8 ± 0.1). Following the pH adjustment, colloid suspension was added to the ^{152}Eu. This gave a total volume of ^{152}Eu/colloid suspension of 300 ml: this volume gives 10 analysis opportunities (triplicates). As all of the colloid suspension was spiked with ^{152}Eu at the same time, control of the contact time between Eu(III) and the colloid is controlled by the removal of the aliquot of solution from the main Eu/colloid mixture and addition of Dowex resin to it. Before the addition of Dowex resin, ^{152}Eu/colloid suspension was removed (10 ml, x3) from the main mixture and placed into a 15 ml tube. Following this, conditioned Dowex was added to the tube (1.4 g) and allowed to rock for 1 hr. After rocking, the sample was centrifuged (15 mins, 4000 rpm) and a 1.5 ml aliquot of the supernatant was removed for gamma ray analysis to measure how much of the Eu(III) was on the Dowex resin (and thus dissociated from the bentonite colloids). Due to the non-destructive nature of gamma ray spectrometry, after measurement, the aliquot can be returned to the sample tube, the resin re-suspended, and the sample put away for later analysis.

Results

Bulk bentonite dissociation

Powder X-ray diffraction was used to show that the EDTA had no effect on the bentonite (data not shown). Figure 3.1.1 shows the dissociation of Eu(III) from bentonite with EDTA contact time as a function of pre-equilibration time of the Eu with the bentonite prior to addition of EDTA.

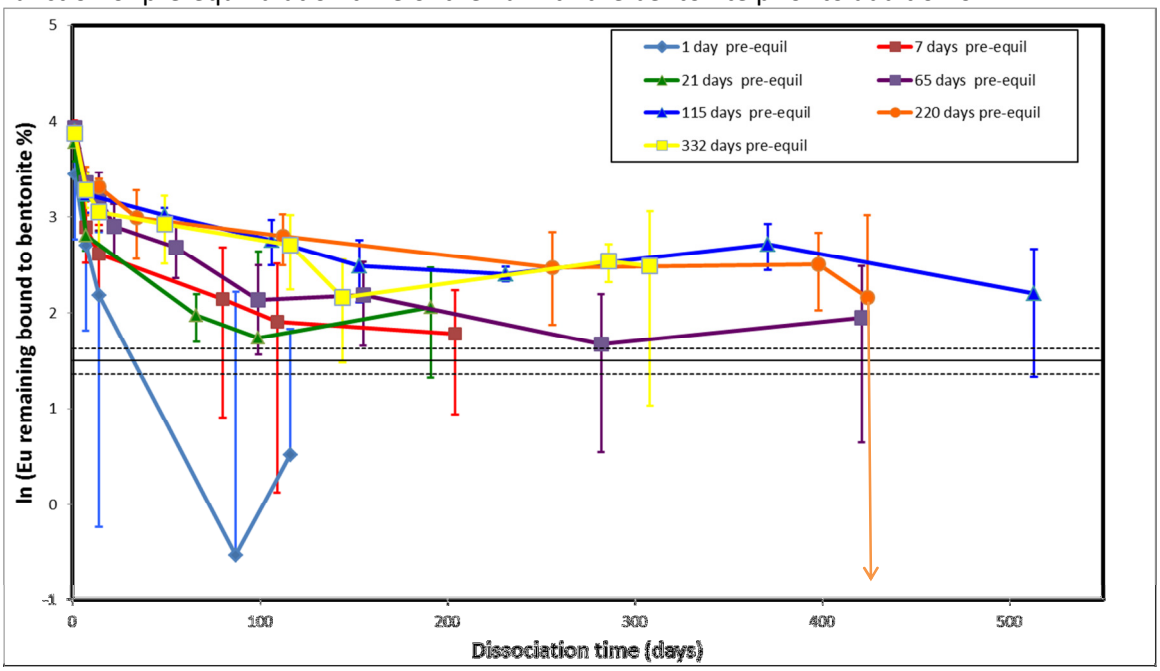

Figure 3.1.1. Natural log of percentage of Eu bound to bentonite vs EDTA contact time, as a function of pre-equilibration time (pH = 7 ± 0.1; I = 0.1 M $NaClO_4$). The full black horizontal line represents the equilibrium position, and the dashed lines represent the experimental uncertainty for the equilibrium position. Errors bars are 2σ based on the standard deviation of triplicate measurements.

The data are plotted as the natural log of the percentage of Eu remaining bound to the bentonite. Eu(III) dissociation followed a similar pattern for all pre-equilibration times. A large part of the Eu(III) (30 - 50 %) dissociated almost instantaneously from the clay.

For the experiments with pre-equilibration times less than 115 days, the Eu distribution between bulk bentonite and EDTA was within error of that at equilibrium between 20 and 100 days. That is, the amount of Eu remaining bound to the bentonite reached the value that would have been observed if the EDTA had been present from the start of the experiment before the Eu was introduced to the clay: This point is shown as the horizontal black line in Figure 3.1. Hence, for these systems, there was no indication of irreversibility. Experiments with pre-equilibration times above 115 days took longer to reach the equilibrium distribution, although all of them had at least one point within error of equilibrium. Therefore, there was no convincing evidence for irreversibility in these systems.

Linear portions of the plots in Figure 3.1.1 indicate a single first order dissociation rate constant, which may be determined from the gradient. Systems with pre-equilibration times greater than 1 day showed different behaviour to that of the 1 day system, where the dissociation was distinctly faster, with a smaller decrease in gradient as EDTA contact time progresses, compared to the other systems. The average dissociation rate constant for this system (taken from day 1 of EDTA contact until the system reaches apparent equilibrium) is approximately 10^{-6} s^{-1}.

For the longer pre-equilibration times, each of the plots shows more than one gradient. There is faster dissociation at the start of the experiment, but after approximately 7 days EDTA contact, there is a distinct reduction in reaction rate. First order dissociation rate constants were calculated by regression for the portions of the plots beyond 7 days of EDTA contact, and the results are shown in Table 3.1.1.

Pre-equilibration Time/day	**Dissociation rate constant (s^{-1})**	**Amount of Eu in slow dissociating fraction with errors (%)**	**τ (Days)**
7	1.01×10^{-7} ($\pm 6.23 \times 10^{-8}$)	17.3 (+3.1; -2.9)	79
21	4.19×10^{-8} ($\pm 8.51 \times 10^{-8}$)	11.9 (+25.2; -4.8)	192
65	3.93×10^{-8} ($\pm 1.35 \times 10^{-8}$)	19.3 (+5.4; -3.5)	204
115	2.17×10^{-8} ($\pm 1.70 \times 10^{-8}$)	20.5 (+8.6; -6.0)	370
220	2.61×10^{-8} ($\pm 1.14 \times 10^{-8}$)	24.3 (+6.7; -5.2)	308
332	2.56×10^{-8} ($\pm 2.87 \times 10^{-8}$)	20.7 (+11.2; -7.3)	314

Table 3.1.1. Dissociation rate constants, reaction half time data and amounts for the most slowly dissociating fraction for Eu and bulk bentonite (pH = 7 ± 0.1; I = 0.1 M $NaClO_4$). Errors are 2σ based on the error determined during regression of the data in Figure 3.1 (due to the log vertical scale in Figure 3.1.1, the errors on the amounts bound are asymmetric).

The amounts of Eu(III) bound to the bentonite in the most slowly dissociating fraction are also shown in Table 3.1.1. There are relatively small differences between the rates for the different systems. The average Eu(III) dissociation rate constant is 4.3×10^{-8} s^{-1}, with a range of 2.2×10^{-8} – 1.0×10^{-7} s^{-1}.

The amount of Eu in the slowly dissociating fraction increases rapidly over the first few days of contact, but beyond 65 days, the amount seems to have reached equilibrium, with around 19 – 25 % slowly dissociating. Virtually all of the Eu in this system (> 96 %) was bound to the bentonite before addition of EDTA: therefore, the other 75 – 81 % of the Eu was bound to the bentonite, but did not get transferred to the slow fraction. This cannot be because it was locked into a different fraction, because it was released instantaneously when EDTA was added. Therefore, in this system, there must be an equilibrium between the Eu in the slowly dissociating and instantaneously available fractions. There is an apparent decrease in the value of the rate constant obtained from regression as pre-equilibration time increases up to 115 days: however, there are large errors on the rate data.

When Eu was first added to the bentonite, it bound quickly, and within the first few hours of contact 96 % of the Eu was bound to the clay. Over the following month, there was a subsequent increase in the amount bound by 3.0 % and an associated increase in the R_d by a factor of 4.1. It is clear that more than this 3.0 % of the Eu changes its interaction with the bentonite, because there is different dissociation behaviour for the system with a short pre-equilibration time and those that were equilibrated for more than 1 day. Therefore, it seems that there is rapid uptake to some fraction that is bound, but may be (relatively) easily removed if a stronger sink becomes available. However, over time it seems that there is a transfer of some of the bound Eu to a fraction that dissociates more slowly. The small increase in R_d suggests that the transfer may also be associated with an increase in thermodynamic stability. However, some of the material (over half in most cases) also remains available for instantaneous dissociation, even after several months of contact time.

Colloid Size Distributions

The colloid and Eu/colloid mixture size distributions are shown in Figure 3.1.2: nominally, the <3 kDa fraction will contain particles no larger than *ca.* 1nm, and so this fraction can be considered as the 'true solution'.

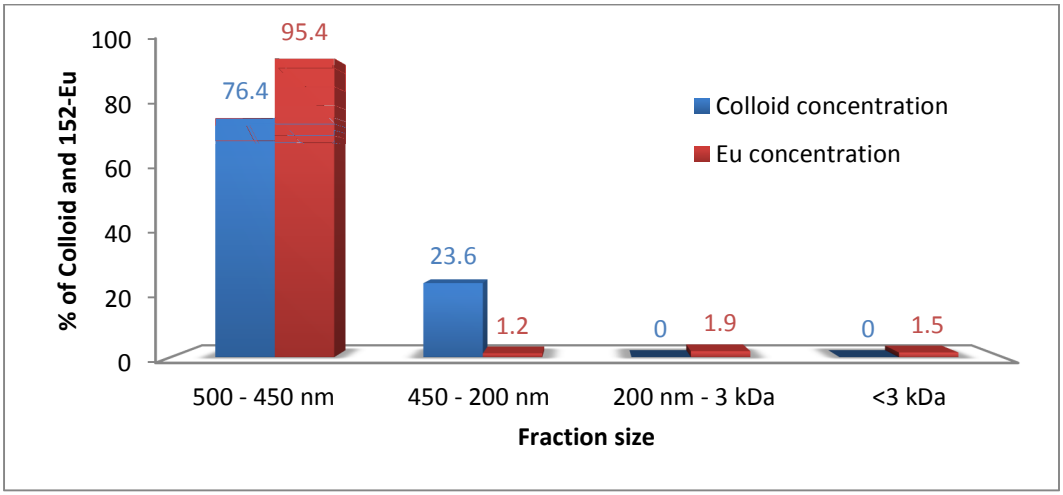

Figure 3.1.2. Colloid and ^{152}Eu(III) concentrations in each size fraction.

The vast majority of the bentonite colloids were in nominal size fractions greater than 200 nm. For the 3kDa – 200 nm fraction, the ratio of Al : Mg (0.62 : 1, with Al = 0.065 ppm and Mg = 0.105 ppm) was far from that of bentonite theoretical value (5.02:1), and so this fraction does not seem to contain significant quantities of bentonite colloids. Also, the Al and Mg concentrations in this fraction were low compared to the others, and so a reliable bentonite colloid concentration could not be calculated. Given that the colloid stock solution had a concentration of 147 ppm, the material responsible for the Al and Mg in the 3kDa – 200 nm fraction represents a very small percentage of the total. The ^{152}Eu(III) showed broadly similar behaviour to that of the colloid, and most of it was bound to the larger colloids (>450 nm; ≈ 95 %). Only 1.5 % of the ^{152}Eu(III) remains in the true solution fraction (<3 kDa). Therefore > 98.5 % of the Eu is colloid associated. The Eu found in the colloidal fraction where no bentonite colloids were detected (3 kDa – 200 nm) was probably due to Eu bound to low concentrations of smaller bentonite colloids that could not be detected or due to other trace colloidal material derived from the bentonite clay, such as quartz. These phases could generate colloids that could bind Eu, but they would not have the expected Al : Mg ratio. Even a very low mass of colloids in the smaller fractions would be particularly reactive, because of their very high specific surface area. Despite this, the amount of Eu observed in the range 3 kDa – 200 nm is small, and so the ^{152}Eu(III) is largely associated with the bentonite colloids.

Eu(III) colloid dissociation

Sodium perchlorate was not added to the colloid experiments, because this would have destabilised the colloids. Instead, the colloid solution was used without alteration. Figure 3.1.3 shows the dissociation of Eu(III) from the bentonite colloids as a function of Eu/colloid pre-equilibration time.

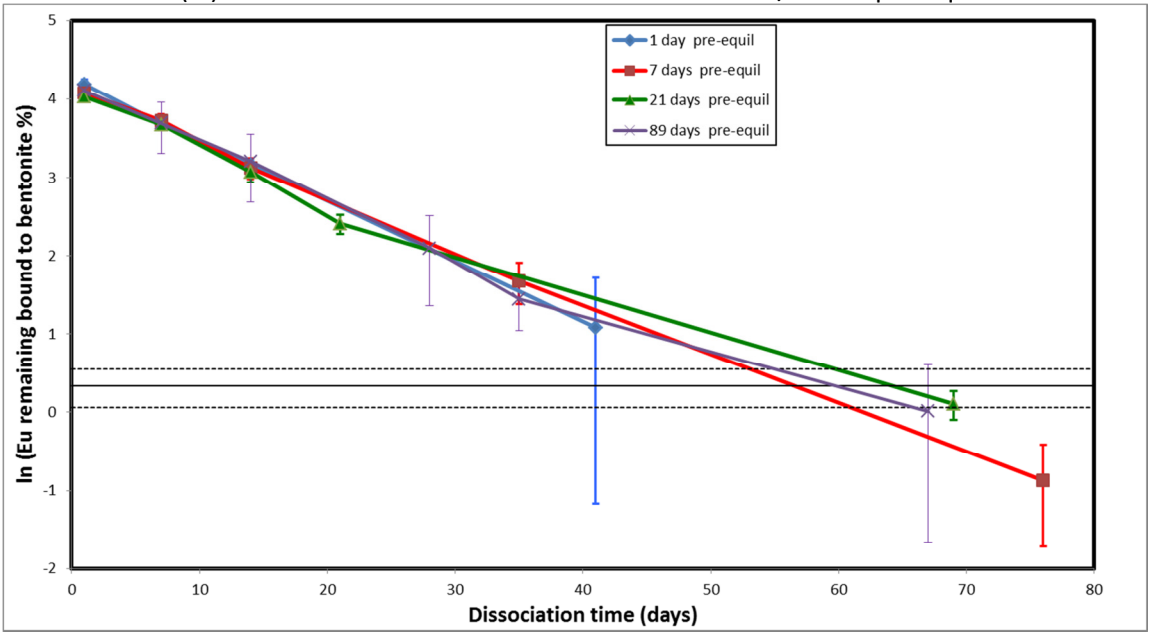

Figure 3.1.3. Natural log plot of the colloid dissociation experiment: ln(percentage bound to bentonite) vs Dowex resin contact times, as a function of pre-equilibration time (pH = 8.8 ± 0.1). The black horizontal line represents the equilibrium distribution, and the dashed lines represent the experimental uncertainty (1.4 ± 1.1 %).

In this system, when the Eu was added to the Dowex resin before the addition of colloids, 1.4 ± 1.1 % remained in solution: this represents the equilibrium position for the colloid experiments (horizontal line, Figure 3.3). For all samples, a similar pattern is observed. A significant part of the Eu(III) (approximately 30 - 40 %) dissociated almost instantaneously from the colloid. This was followed by slower dissociation over time.

The dissociation observed for the colloids was very different to that of the bulk bentonite. More Eu is found in the slowly dissociating fraction, and there is no increase in the amount bound beyond 1 day pre-equilibration time. Further, beyond the initial rapid dissociation, only a single rate constant is observed throughout the duration of the experiment. First order dissociation rate constants and the amounts in the most slowly dissociating component were calculated by regression, and the results are shown in Table 3.1.2.

Pre-equilibration System/day	Dissociation rate constant (s^{-1})	Amount of Eu in fraction (%)	τ (Days)
1	8.97×10^{-7} ($\pm 2.27 \times 10^{-8}$)	69.8 (+3.1; -2.9)	8.94
7	7.66×10^{-7} ($\pm 5.63 \times 10^{-8}$)	60.8 (+12.4; -10.3)	10.5
21	9.47×10^{-7} ($\pm 2.63 \times 10^{-7}$)	64.9 (+22; -17)	8.47
89	9.04×10^{-7} ($\pm 2.55 \times 10^{-8}$)	69.2 (+11; -9.5)	8.87

Table 3.1.2. Dissociation rate constants, reaction half time data and amounts for the most slowly dissociating fraction (pH = 8.8 ± 0.1). Note, calculating an overall rate for all data in Figure 3.3 gives an average first order rate constant of 8.8×10^{-7} s^{-1}. Errors are 2σ based on the error determined during regression of the data in Figure 3.3 (due to the log vertical scale in Figure 3, the errors on the amounts bound are asymmetric).

The dissociation rate constants for the colloids are over an order of magnitude higher than for the bulk sample. The reasons for the differences are uncertain, but it could be due to the narrow size distribution of the bentonite colloids making the system more homogenous than bulk experiments (Figure 3.1.2). Beyond being more heterogeneous in terms of particle size, as a natural material, the bulk sample is also more chemically heterogeneous too. It seems likely that both of these factors contribute to the difference.

The binding of Eu(III) to bentonite in this experiment was similar to that reported in the literature. Missana et al. (2008) and Bouby et al. (2011) found that it would associate to the clay, but in the presence of a competitor, it would dissociate. Bouby et al. (2011) used humic acid as a competitor and reported that on addition of humic acid an instantaneous, partial dissociation of the radionuclide from the bentonite occurred. The same was observed in these experiments, since on initial addition of EDTA/resin at least 30 % of the Eu dissociates immediately.

Wold (2010) estimated dissociation rate constants for some metal ions (see values above). These values were calculated from K_d values and association rates. We might expect some differences between the values reported here and those of Wold (2010), because Wold's calculation assumes that all of the bentonite bound radionuclide represents a single fraction, whereas, the kinetic data for the bulk and colloidal experiments (Figures 3.1 and 3.3) show at least 3 and 2 fractions, respectively. Wold's rate constant for Am(III) (5.6×10^{-7} s^{-1}) is an order of magnitude higher than that recorded here for the bulk (4.3×10^{-8} s^{-1}). The other trivalent rate constant from Wold (2010), Cm(III) (1.7×10^{-6} s^{-1}), is also higher than the Eu bulk experiment rate here (4.3×10^{-8} s^{-1}). However, the colloid rate constants observed here fall within the range of trivalent rate constants reported by Wold (2010). Huber et al. (2011) have also provided dissociation rate constants for bentonite colloids from competition experiments using fracture filling material. For Am(III), the values were in the range 1 - 2.5×10^{-6} s^{-1}, whilst for Pu(IV), the range was 3.9×10^{-7} - 2.4×10^{-6} s^{-1}. The bulk rate constants in this study are lower than the data from Huber et al. (2011) (Table 3.1), but again the colloidal values are much closer (Table 3.2).

At present, the mechanism responsible for the slow dissociation is uncertain. For a lanthanide ion, such as Eu(III), we would not automatically expect dissociation from a surface complexation site to be so slow. Therefore, it seems that there must be some other mechanism responsible for the slow dissociation. In the case of some radionuclides and concentrations, it has been suggested that surface precipitation could be responsible, particularly for tetravalent ions (Bouby et al. 2011). However, it seems less likely that is the case for a trivalent radionuclide, such as Eu(III), especially given the low concentrations of Eu and the ambient pH studied here. Metal ions do diffuse into the interlayer spaces of clay structures, and it is possible that this is partly responsible for the slow dissociation: this might explain the difference between the bulk and colloidal Eu(III) rate constants, since the particles will be smaller for the colloid system, and so the extent to which a metal ion could get hidden inside the structure could be reduced, giving a faster dissociation rate. Clearly, additional work is required to deduce the mechanism of interaction more fully.

3.2 U/Bentonite systems

The authors involved in the work in this section are: N. Sherriff, F, Livens (*Centre for Radiochemistry Research, School of Chemistry, University of Manchester, Manchester, U.K.*) and N.D. Bryan (*National Nuclear Laboratory, 5th Floor, Chadwick House, Birchwood, Warrington, WA3 6AE, UK*).

In these experiments, the interaction of uranium with bentonite has been studied.

3.2.1 Materials and Methods

The clay used in this work is a sodium Wyoming bentonite. All water was deionised (18 MΩ) and all reagents were analytical grade. All experiments were repeated in triplicate.

Colloid studies

Colloid Formation

Colloid formation was performed as in the europium work in Section 3.1.

^{232}U(VI) purification

^{232}U(VI) was obtained through separation using a 2 ml UTEVA resin column purchased from Eichrom. The column is supplied pre-conditioned in HCl (0.1 M), and was re-conditioned with HCl washes (5 M, 3 x 5 ml). Before separation, the ^{232}U(VI) was in radioactive equilibrium with ^{228}Th(IV). The untreated ^{232}U(VI) (2 ml, 8 kBq ml^{-1}) sample was adjusted to an HCl concentration of 5 M (with a total final volume of 20 ml). This solution was passed through the column. At this HCl concentration, the ^{228}Th(IV) passed through the column and the ^{232}U(VI) was retained. The ^{232}U(VI) was then eluted using HCl (0.1 M, 16 ml) to give a pure solution of ^{232}U(VI) (16 ml, 1 kBq ml^{-1}).

Uranium/bentonite colloid association

^{232}U(VI) (4 ml, 1 kBq ml^{-1}) was adjusted to pH 8.8 ± 0.2, colloid suspension (4 ml, 171 ppm) was added, and the ^{232}U(VI)/colloid suspension (8 ml, 0.5 kBq ml^{-1}) was allowed to equilibrate for 24 hrs. Syringe filters (450 nm, 200 nm and 100 nm) polyether sulphone (PES) membranes were used to filter the ^{232}U(VI)/colloid suspension. The filters were first equilibrated for 68 hrs to the pH of the ^{232}U(VI)/colloid suspension (8.8 ± 0.2). A separate filter was exposed to the ^{232}U(VI)/colloid suspension to test whether the filters themselves sorbed the ^{232}U(VI); less than 1 % of the ^{232}U(VI) was sorbed by the filter.

Speciation calulations

Solution speciation was calculated with PHREEQCi (Parkhurst et al. 1999), using the ThermoChimie v.7.b database (Duro et al 2006, Grive et al, 2010).

Dissociation experiments

Dowex 50WX4-200 (H-form) resin was converted to its sodium form. 20 g of Dowex resin were added to a sintered column, and washed with: deionised water (150 ml); HCl (2 M, 500 ml); deionised water (500 ml); NaCl (3 M, 500 ml); NaOH (0.1 M, 500 ml); and finally deionised water (500 ml). Experiments showed that the colloid did not interact with the pH pre-conditioned resin (data not shown).

^{232}U(VI) solution (15 ml, 15 kBq) was added to a container and its pH was adjusted to 8.8 ± 0.1). After pH adjustment, colloid suspension (135 ml, 171 ppm) was added to the ^{232}U(VI) to give an overall ^{232}U(VI)/bentonite colloid solution of 150 ml ([^{232}U] = 100 Bq ml^{-1}, 5.43×10^{-10} M; [colloid] = 171 ppm). Aliquots from this main solution were then removed at different pre-equilibration times (3 x 10 ml), and to these conditioned Dowex resin was added (1.4 g). The samples were then allowed to rock

gently for 1 hr before being centrifuged (15 mins, 4000 rpm, RCF = 2504) and a 0.1 ml aliquot was removed for ^{232}U(VI) analysis. The samples were returned to storage and further aliquots were taken at intervals.
^{232}U(VI) analysis was performed via scintillation counting on a 1220 QUANTULUS ultra-low level scintillation spectrometer. Scintisafe 3 (purchased from Fisher) was added to the samples (10 ml), followed by deionised water (0.9 ml), HCl (1 M, 1 ml), and finally the sample (0.1 ml). The mixtures were shaken vigorously for 30 seconds and allowed to settle for 24 hrs before analysis.

Results

^{232}U(VI)/Bentonite colloid association

Previous studies (Bouby et al. (2010), Bouby et al. (2011), Mori et al. (2003), Huber et al. (2011)) have indicated that there is little or no association of U(VI) to bentonite colloids (U(VI) concentrations of 1×10^{-7}, 4.2×10^{-8}, 8.69×10^{-7} and 4.3×10^{-7} M, respectively). Filtration experiments were performed to measure the amount of U(VI) that was colloid bound. Sequential filtrations of the colloid stock and the ^{232}U(VI)/colloid suspension were performed through 450, 200 and 100 nm PES filters. The results are shown in Figure 3.2.3.

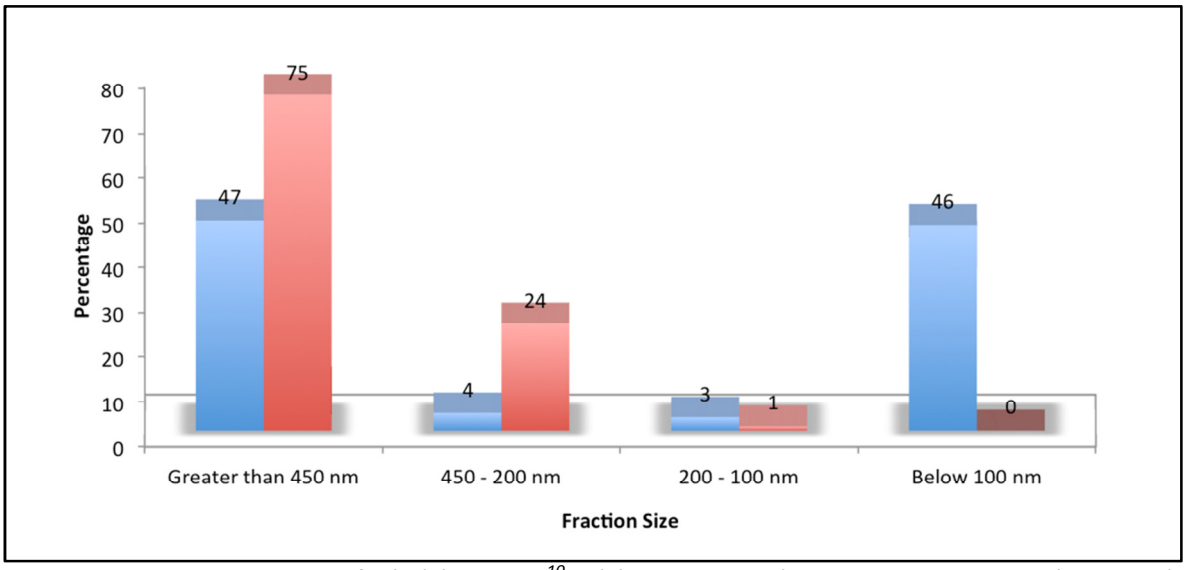

Figure 3.2.3. A comparison of U(VI) (3.38×10^{-10} M) (blue columns) and bentonite colloid (171 ppm) (red columns) filtrates at pH 8.8

The colloid size distribution (red columns) shows 75 % in the greater than 450 nm fraction, 24 % in 450 – 200 nm, 1 % in the 200 – 100 nm fraction, and 0 % in the below 100 nm fraction, which is consistent with the SEM images (Figures 3.2.1 and 3.2.2). The U(VI) (blue columns) has 47 % in the >450 nm fraction, 4 % in the 450 -200 nm fraction and 3 % in the 200 – 100 nm fraction, with 46 % in the <100 nm fraction. In the absence of bentonite colloids, no uranium is found in the >100 nm fraction, showing that approximately 54 % of the uranium is bentonite colloid associated. The 46 % in the <100 nm fraction cannot be associated with the bentonite colloids, as none were found in this size range. Bouby et al. (2010), Bouby et al. (2011) and Mori et al. (2003) found a much smaller amount of U associated to the bentonite colloids (5.8 %, 6 % and 6 %, respectively). However, in their experiments they use U concentrations of 4.3×10^{-7} M, 4.2×10^{-8} M and 8.69×10^{-7} M, respectively, and 20 ppm colloid suspensions, whereas in this study the U concentration is 3.38×10^{-10} (two to three orders of magnitude less) and a 171 ppm colloid suspension (nearly 9 times the amount used in the other studies). The differences in experimental conditions could explain the differences seen in

the association of U to bentonite colloids. It could be possible that a saturation level has been reached in the other studies, which could explain the apparently lower affinity.
For the size fractions where bentonite colloids are present (> 100 nm), the amount of uranium bound per mass of colloid decreases with increasing colloid fraction size. This is expected, since the smaller colloids will have the higher specific surface area, and hence mass for mass more binding sites.

Speciation calculations
Speciation modelling was performed for the U(VI) and the results can be seen in Table 3.2.1. The speciation calculations do not include any uranium that is colloid associated, in the true system some uranyl is colloid associated (Figure 3.2.3), but the thermodynamic database does not contain parameters for U(VI)/bentonite interactions. Hence, the speciation in Table 3.2.1 represents the true solution speciation.

Species	**% in sol.**
$UO_2(CO_3)_3^{-4}$	97.00
$UO_2(CO_3)_2^{-2}$	2.95
$UO_2(OH)_3^-$	1.06×10^{-2}
$UO_2(CO_3)$	5.47×10^{-03}
$UO_2(OH)_2$	1.99×10^{-03}
$UO_2(OH)^+$	2.67×10^{-05}
$UO_2(OH)_4^{-2}$	5.75×10^{-06}
$UO_2SiO(OH)_3^+$	2.34×10^{-06}
$(UO_2)_2(CO_3)(OH)_3^-$	8.88×10^{-07}
UO_2^{+2}	9.12×10^{-09}

Table 3.2.1. Uranium speciation (excluding colloid associated U),U(VI) 5.43 x 10^{-10} M, pH 8.8, assuming equilibrium with atmospheric CO_2 and montmorillonite

97 % of the uranium in the solution is present as $UO_2(CO_3)_3^{-4}$ and 2.95 % as $UO_2(CO_3)_2^{-2}$. Overall, 99.95 % of the uranium species in this system is complexed with carbonate. The aqueous U(VI) species are in equilibrium with the U(VI) species bound to the colloid surface. Despite the strength of the interaction with carbonate, 54 % of the uranyl is colloid bound, even though the amount of free uranyl is small (9.12×10^{-09} %). This could be an indication that the intrinsic interaction of uranyl with bentonite binding site is relatively strong.

^{232}U(VI) Dissociation from bentonite colloids
The principle underlying the dissociation experiment was that, of the U(VI) added to the system, 54 % would bind to the bentonite colloid (as shown in the filtration studies) and 46 % would remain in the solution. Please note that the percentages in is the text below refer to the total element concentration in the systems (sum of element bound and element in solution), i.e., the dissociation is discussed in terms of the total U in the system. When the U/bentonite colloid system was interacted with Dowex, the 46 % in the true solution is removed rapidly. Anyslow dissociation must be due to the U associated with the colloids.
Figure 3.2.4 shows the dissociation of U(VI) from bentonite colloids as a function of U/colloid pre-equilibration time.

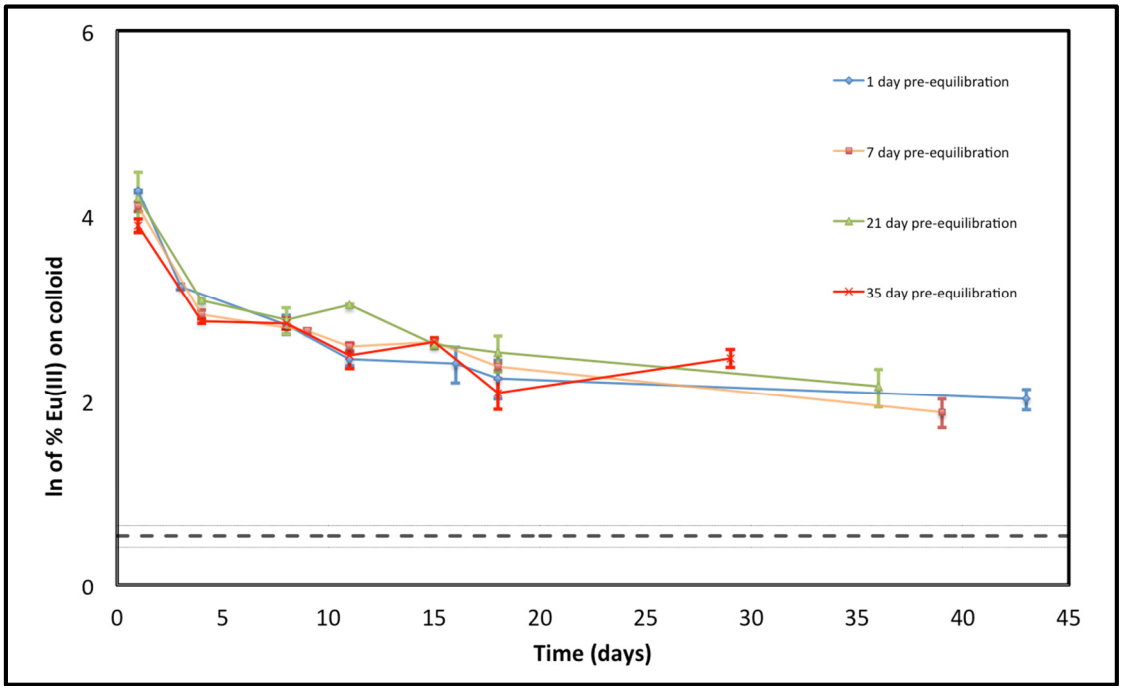

Figure 3.2.4. Natural log plot of the colloid dissociation experiment: ln(percentage ([U] = 5.43 x 10^{-10} M) bound to bentonite) vs time (days), pH = 8.8 ± 0.2. The dashed black horizontal line represents the equilibrium distribution, and the thin lines represent the experimental uncertainty (1.7±0.2 %)

In a separate experiment, U was added to the Dowex resin before the addition of bentonite colloid suspension. In that system, at equilibrium, 1.7 ± 0.2 % of the U was in solution. This represents the position of equilibrium for the experiments shown in Figure 3.2.4 (the dashed horizontal line in Figure 3.2.4). In the absence of bentonite colloids, the uranyl is removed from the solution by the resin within 48 hrs.

On initial contact with the Dowex resin there is an instantaneous reduction in the amount of U in solution (approximately 30-50 %). The filtration experiment showed that approximately 46 % of U(VI) is not bound to the bentonite colloids, and the instantaneous reduction of U(VI) from the solution is consistent with that figure, and so most of the initial rapid drop is probably due to removal from solution of the uranium not associated with the bentonite colloid.

Analysis after 4 days of contact time shows 25.3 ± 0.80 %, 18.6 ± 0.9, 21.8 ± 0.4 % and 17.3 ± 0.4 % for pre-equilibration times of 1, 7, 21 and 35 days, respectively, with an average of 20.8 % U remaining in solution. From this point on, the plots for the different equilibration times show broadly similar behaviour to each other. The gradient is steeper between days 1 and 4, than the remainder of the experiment, which is an indication of more than one dissociation rate. This fraction accounts for approximately 30% of the U in the system. Beyond day 4, there is slower dissociation of the remainder of the U. First order rate constants and the amount of uranium in the most slowly dissociating fraction were calculated by linear regression, and the results are given in Table 3.2.2.

Pre-equilibration System/day	Dissociation rate constant (s^{-1})	Amount of U in fraction (%)	τ (Days)
1	7.8×10^{-7} ($\pm 5.8 \times 10^{-7}$)	27.9 (+24.3; -13.0)	11
7	3.1×10^{-7} ($\pm 1.6 \times 10^{-6}$)	20.4 (+69.7; -15.8)	25.8
21	4.6×10^{-7} ($\pm 2.4 \times 10^{-7}$)	24.9 (+7.2; -5.6)	17.4
35	6.9×10^{-7} ($\pm 9.0 \times 10^{-7}$)	23.7 (+33.8; -14.0)	11.7

Table 3.2.2. Dissociation rate constants, reaction half time (τ) data and amounts for the most slowly dissociating fraction (pH = 8.8 ± 0.1). Note, calculating an overall rate for all data in Figure 4.4 gives an average first order rate constant of 5.6 x 10^{-7} s^{-1}. Errors are 2σ based on the error determined during regression of the data in Figure 3.2.4.

The average dissociation rate constant for the data in Table 4.2 is 5.6×10^{-7} s^{-1} ($\pm 4.2 \times 10^{-7}$). The lack of kinetic data for U(VI) dissociation from bentonite colloids in the literature, makes comparisons difficult. Wold (2010) calculated a first order U(VI) dissociation rate constant from K_d values of 8.3 x 10^{-7} s^{-1}. The experimental values in Table 3.2.2 are similar. The overall rate constant is within error of the value estimated by Wold (2010), and three of the individual values in the table are also within error (only the 21 day system is outside).

The europium studies in Section 3.1 measured a dissociation rate constant in a similar experiment using Eu(III) ((8.8 ± 9.1)x 10^{-7} s^{-1}). The U(VI) rate constant measured here is within experimental error of this value.
Section 3.1 showed that beyond an initial rapid dissociation in the Eu(III)/bentonite colloid studies, only a single slow dissociation rate constant was observed. With U however, there is evidence of a two-step slow dissociation from the bentonite colloids.

The average amount of U(VI) in the most slowly dissociating fraction is approximately 24 ± 6.2 % of the U inventory. Section 3.1 reports an average amount for Eu(III) of 66 ± 8.4 % in the most slowly dissociating fraction, but in that system, approximately 100 % of the Eu(III) is associated with the bentonite colloids. Taking into account that only 54 ± 6 % of the U is colloid associated explains why there is less U in the most slowly dissociating fraction when compared to the similar Eu experiments from Section 3.1..
Because there is evidence of a two-step dissociation, then it is likely that the uranyl ion is bound to the bentonite colloid in two different ways. The initial dissociation (day 1 – 4) observed is possibly U(VI) that is more available for dissociation (probably surface bound). The slower dissociating U(VI) could be less available for dissociation possibly because of a speciation change on the colloid surface or integration into the colloid layers.
Bouby et al. (2010), Bouby et al. (2011), Mori et al. (2003) found only small amounts of U bound (5.8 %, 6 % and 6 % respectively) compared to this study (54 %). The U concentrations used in those studies (4.3 x 10^{-7} M, 4.2 x 10^{-8} M and 8.69 x 10^{-7} M respectively) were two to three orders of magnitude more than used in this study). In such systems, the slow dissociation would be difficult to observe.

The mechanism responsible for the slow dissociation of the U(VI) from bentonite is unknown at present. Slow dissociation could reflect several possible effects, from surface precipitation (Bouby et al. 2011) to integration into the clay layers (Section 3.1). The fact that both U(VI) and Eu(III), with their very different chemistries, show very similar rate constants could suggest that there is a common mechanism, but U shows at least 2 slow dissociating steps and Eu only shows 1. It has been

suggested that slow dissociation of surface complexes could explain the slow dissociation. If this were the case, then we might expect that their dissociation rate constants would be different due to the different chemical interactions with the bentonite.

3.3 Am and Th/Bentonite systems

The authors involved in the work in this section are: N. Sherriff, F, Livens (*Centre for Radiochemistry Research, School of Chemistry, University of Manchester, Manchester, U.K.*) and N.D. Bryan (National Nuclear Laboratory, 5th Floor, Chadwick House, Birchwood, Warrington, WA3 6AE, UK).

In these experiments, the interaction of thorium and americium with bentonite has been studied.

3.3.1 Materials and Methods

The clay used in this work is a sodium Wyoming bentonite. All water was deionised (18 MΩ) and all reagents were analytical grade. All experiments were repeated in triplicate.

Colloid studies

Colloid Formation

Colloid formation was performed as in the europium work in section 3.1.

^{228}Th(IV) purification

^{228}Th(IV) was obtained through separation using a 2 ml UTEVA resin column (Eichrom). The column comes pre-conditioned in HCl (0.1 M), and was re-conditioned with HCl (5 M, 3 x 5 ml) washes. Before separation, the ^{228}Th(IV) was in equilibrium with ^{232}U(VI). The untreated ^{232}U(VI)/ ^{228}Th(IV) (2 ml, 8 kBq ml^{-1}) sample was adjusted to a HCl concentration of 5 M (20 ml). This solution was passed through the column. At this HCl concentration, the ^{228}Th(IV) passed through the column and the ^{232}U(VI) was retained. A further wash with HCl (5 M, 15 ml) gave a U(VI) free ^{228}Th(IV) solution (35 ml, 230 Bq ml^{-1}).

Thorium/bentonite colloid association

^{228}Th(IV) (4 ml, 230 Bq ml^{-1}) was adjusted to pH 8.8 ± 0.2, colloid suspension (6 ml, 171 ppm) was added and the ^{228}Th(IV)/colloid suspension (10 ml, 92 Bq ml^{-1}) allowed to equilibrate for 24 hrs. Syringe filters (450 nm, 200 nm and 100 nm PES filters) were used to filter the ^{228}Th(IV) /colloid suspension. The filters were first equilibrated for 68 hrs to the pH of the ^{228}Th(IV) /colloid suspension (8.8 $\pm$ 0.2). Separate filters were exposed to the ^{228}Th(IV)/colloid suspension. It was found that 9.3 ± 6.1 % sorbed to the filter.

Americium/bentonite colloid association

^{241}Am(III) (0.1 ml, 10 kBq ml^{-1}) was added to DI water (0.9 ml) and the pH adjusted to 8.8 ± 0.2. Colloid suspension (19 ml, 171 ppm) was added to this and the ^{241}Am(III)/colloid suspension (20 ml, 50 Bq ml^{-1}) was allowed to equilibrate for 24 hrs. Syringe filters (450 nm and 200 nm PES filters) were used to filter the ^{241}Am(III)/colloid suspension. The filters were first equilibrated for 68 hrs at the pH of the ^{241}Am(III)/colloid suspension (8.8 ± 0.2). Separate filters were exposed to the ^{241}Am(III)/colloid suspension to see if the filters themselves competed for the ^{241}Am(III), but <1 % of the ^{241}Am(III) sorbed to the filters.

Speciation calculations

Solution speciation was calculated with PHREEQCi (Parkhurst et al. 1999), using the ThermoChimie v.7.b database (Duro et al 2006, Grive et al, 2010).

Dissociation experiments

Cellulose phosphate (Cellphos) was purchased from Sigma-Aldrich. 20 g was added to DI water (100 ml) and equilibrated to pH 8.8 for 24 hours with stirring. The DI water was decanted and the Cellphos was placed on a watch glass and air-dried before being stored in a plastic screw top container (Li, 2011). The colloid did not interact with the pre-conditioned resin (data not shown).
^{228}Th(IV) solution (1.5 ml, 4 kBq) was added to a container and its pH was adjusted to 8.8 ± 0.1. After the pH adjustment, colloid suspension (148.5 ml, 171 ppm) was added to the ^{228}Th(IV) to give a ^{228}Th(IV)/bentonite colloid mixture of 150 ml (26.7 Bq ml^{-1}, 3.79 × 10^{-12} M). Aliquots from this main solution were then removed at different pre-equilibration times (3 x 10 ml at each time point) and, to these, conditioned Cellphos was added (1 g). The samples were then allowed to rock gently for 1 hr before being centrifuged (15 mins, 4000 rpm, RCF = 2504) and a 0.1 ml aliquot was removed for ^{228}Th(IV) analysis. The samples taken for analysis were stored for 28 days to equilibrate with the ^{228}Th(IV) daughter products.
^{228}Th(IV) analysis was performed via scintillation counting on a 1220 QUANTULUS ultra-low level scintillation spectrometer. Scintisafe 3 (Fisher) was added to the samples (10 ml), followed by DI water (0.9 ml), HCl (1 M, 1 ml), and finally the sample (0.1 ml). The mixtures were shaken vigorously for 30 seconds and allowed to equilibrate for 28 days before analysis.
^{241}Am(III) solution (1.5 ml, 15 kBq) was added to a container and its pH was adjusted to 8.8 ± 0.1. After pH adjustment, colloid suspension (148.5 ml, 171 ppm) was added to the ^{241}Am(III) to give an overall ^{241}Am(III)/bentonite colloid mixture of 150 ml (100 Bq ml^{-1}, 3.27 × 10^{-9} M). Aliquots from this main solution were then removed at different pre-equilibration times (3 x 10 ml for each sample point) and conditioned Cellphos was added (0.2 g). The samples were then allowed to rock gently for 1 hr before being centrifuged (15 mins, 4000 rpm, RCF = 2504) and a 1.5 ml aliquot was removed for ^{241}Am(III) analysis via gamma-ray spectrometry.
^{241}Am(III) analysis was performed on a lead/copper shielded gamma ray spectrometer (Canberra 2020 coaxial HPGe gamma spectrometer with an Ortec 919E multi-channel analyser). The samples were placed in identical containers and counted for 30 minutes before being returned to the experiment.

Results and discussions

^{228}Th(IV) and ^{241}Am(III)/bentonite colloid association

Previous studies (Bouby et al. (2010), Bouby et al. (2011), Mori et al. (2003), Huber et al. (2011)) showed that Th(IV) is strongly associated to the bentonite colloids. It is, however, likely that a significant proportion of Th(IV) actually forms radiocolloids before any interaction with bentonite colloids; for example Mori et al. (2003) measured 20 – 30 % of Th(IV) ([Th] = 1.12 × 10^{-8} M) in the colloidal fraction before any interaction with bentonite colloids. The same studies have also shown that Am(III) (or, in the case of Bouby et al. (2010), Eu(III) as an analogue) is also strongly bound to bentonite colloids, while Mori et al. (2003) measured 6 -58 % of Am(III) ([Am] = 5.4 x 10 $^{-9}$ mol L^{-1}) in the colloidal fraction before introduction of the bentonite colloids.
Here, the colloid stock was filtered sequentially through 450, 200 and 100 nm PES filters, and each filtrate was then analysed for colloid content by ICP-AES. ^{228}Th(IV)/colloid and ^{241}Am(III)/colloid suspensions were filtered separately and analysed for Th(IV) and Am(III) content. These data were then combined to show the amount of radionuclide that is colloid-associated in the two systems, and the results are shown in Figure 3.3.1.

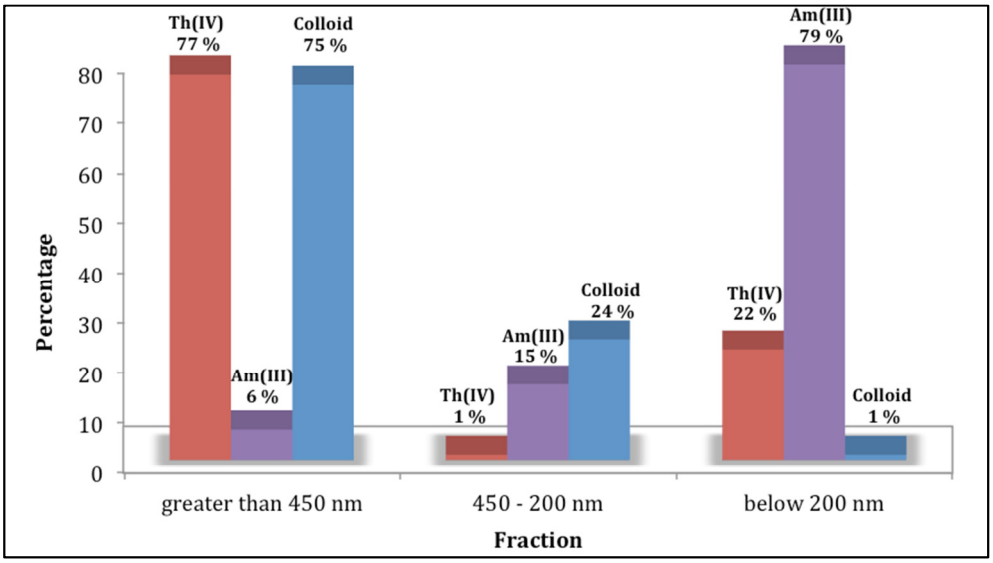

Figure 3.3.1. Comparison of Th(IV) (1.31 x 10^{-12} M), Am(III) (3.27 x 10^{-9} M) and bentonite colloid solution (171 ppm) filtrates at pH 8.8.

As can be seen in Figure 3.3.1, the bentonite colloid size distribution shows 75 % in the >450 nm fraction, 24 % in 450 – 200 nm and 1 % in the <200 nm fraction, consistent with previous date in Sections 3.1 and 3.2, which showed that there were no detectable colloids below 100 nm.
Th(IV) is distributed 77 % in the >450 nm fraction, followed by 1 % in the 450 -200 nm fraction and 22 % in the <200 nm fraction. Approximately 78 % of the Th(IV) is found in the > 200 nm fraction, which is where 99 % of the bentonite colloids are detected. As only 1 % of the bentonite colloids are below 200 nm (no bentonite colloids detected <100 nm), then the remaining 22 % of Th(IV) cannot be bentonite colloid associated.
Mori et al. (2003) showed that even before the addition of bentonite colloids 20 – 30 % of the Th(IV) was in the colloidal fraction. Previous work, e.g., Ekberg et al. (1999) has shown that Th(IV) forms polymeric and colloidal species Below 200 nm, there is a very small bentonite colloid concentration (1 %), and so it is possible that the Th(IV) in this fraction (22 %) is not associated with bentonite colloids, and may be present as intrinsic Th(IV) colloids or some other polymeric species As such, it could be unavailable for binding to the bentonite colloids.
Only 6 % of the Am is in the >450 nm fraction, followed by 15 % in the 450 -200 nm fraction and 79 % in the <200 nm fraction. Of the Am(III) in the suspension, it seems that 21 % of the Am at most is bentonite colloid associated.
Mori et al. (2003) showed that even before the addition of bentonite colloids, 6 – 58 % of the Am(III) was in the colloidal fraction. Further, Ijima et al. (2010) showed that in certain systems, radiocolloids of Am are formed, and that their formation can affect Am behaviour.
Below 200 nm there is a very small bentonite colloid concentration (1 %), and since Am can form intrinsic radiocolloids (Ijima et al. 2010) and that the amount of Am in the colloidal fraction has been measured at approximately 60 % in similar conditions (Mori et al. 2003), then it seems likely that the 79% of Am in the < 200 nm fraction is not associated with bentonite colloids.

Speciation calculations

Speciation modelling was performed for the Th(IV) and Am(III) and the results can be seen in Tables 3.3.1 and 3.3.2, respectively. The speciation calculations do not include any metal that is colloid associated, either bound to bentonite colloids or in the form of intrinsic colloids. The data represent only the composition of the true solution phase.

Species	% sol.
$Th(OH)_3(CO_3)^{-1}$	59.6
$Th(OH)_2(CO_3)_2^{-2}$	32.3
$Th(OH)_4$	7.88
$Th(OH)_2(CO_3)$	0.14
$Th(OH)_4(CO_3)^{-2}$	5.74×10^{-02}
$Th(OH)_3^{+1}$	3.35×10^{-02}
$Th(OH)(CO_3)_4^{-5}$	9.98×10^{-03}
Th^{+4}	1.25×10^{-17}

Table 3.3.1. Thorium speciation (excluding colloid associated), Th(IV) 5.43×10^{-10} M, pH 8.8, assuming equilibrium with atmospheric CO_2 and montmorillonite

Species	% sol.
$Am(CO_3)_2^-$	79.7
$Am(CO_3)^+$	17.8
$Am(CO_3)_3^{-3}$	1.23
$Am(OH)_2^+$	0.80
$AmOSi(OH)_3^{+2}$	0.32
$Am(OH)^{+2}$	0.12
$Am(HCO_3)^{+2}$	1.18×10^{-02}
Am^{+3}	4.35×10^{-03}

Table 3.3.2. Americium speciation (excluding colloid associated), Am(III) 3.27×10^{-9} M, pH 8.8, assuming equilibrium with atmospheric CO_2 and montmorillonite

59.6 % of the thorium species formed in the system is $Th(OH)_3(CO_3)^{-1}$, 32.3 % is $Th(OH)_2(CO_3)_2^{-2}$ and, overall, 91.9 % of the thorium species in this system are hydroxy carbonate complexes and 7.9 % of the thorium is present as the neutral thorium hydroxide species.
79.7 % of the americium species formed in the system is $Am(CO_3)_2^-$, 17.8 % is $Am(CO_3)^{1+}$ and 1.23 % is $Am(CO_3)_3^{-3}$.
PHREEQC modelling also provided saturation indices for the phases in the Th(IV) and Am(III) systems. The ThermoChimie database contains solubility products for different phase types: colloid (coll), crystalline (cr), microcrystalline (mcr) and amorphous (am).. Crystalline forms are expected to take a long time to form in a system, whereas microcrystalline and particularly amorphous species could form much quicker. A negative saturation index indicates under saturation and a positive value indicates super-saturation. The relevant saturation indices of Th and Am are shown in Table 3.3.3, and Eu is included for comparison to Am.

Species	Phase type	Saturation Index
ThO_2	coll	-6.22
ThO_2	cr	3.11
ThO_2	mcr	1.88
$Am(CO_3)(OH)$	am	2.84
$Am(OH)_3$	am	1.39
$Eu(CO_3)(OH)$	cr	0.40
$Eu(OH)_3$	am	-5.18
$Eu(OH)_3$	cr	-3.04

Table 3.3.3. Relevant saturation values for Th(IV) and Am(III) in the systems, a positive value indicates super-saturation, with the relevant saturation types. The Eu(III) saturation indices from the analogous studies in section 3.1 of this report are shown for a comparison to Am(III)

The Th(IV) system has a negative value (-6.22) for the formation of radiocolloids (coll), which is an indication that radiocolloids of Th(IV) should not form in this system. However, the saturation indices are positive for ThO_2 in both the crystalline (cr = 3.11) and microcrystalline (mcr = 1.88) forms, indicating super-saturation of these species. It is expected that crystalline types will take a long time to form, but it is possible that microcrystalline or partially amorphous species could form sufficiently quickly in the initial solution to have an effect on the binding of Th(IV) to the bentonite colloids.
The Am(III) in these studies shows a weak affinity for the bentonite colloids (maximum 21 % association). However, its notional analogue Eu(III) showed a strong affinity for the bentonite colloids (nearly 100 % association). Table 3.3.3 shows the saturation indices of the Am(III) in this study and the saturation indices of the Eu(III) for the experiments described in Section 3.1. It can be seen that for the Am(III) both amorphous $Am(CO_3)(OH)$ and amorphous $Am(OH)_3$ are to super-saturated (saturation indices of 2.84 and 1.39, respectively). Amorphous products can form quickly, and it is likely that these amorphous products form in these systems. This does not happen in the Eu(III) systems. Amorphous $Eu(OH)_3$ has a negative saturation index (-5.18) and so is not expected to form. Crystalline $Eu(OH)_3$ has a negative saturation value (-3.04) and so is not expected to form. Crystalline $Eu(CO_3)(OH)$ does have a positive value (0.40), but may form relatively slowly. The saturation data help to explain the poor binding affinity of Am(III) to bentonite colloids and the differences between Eu(III) and Am(III).

^{228}Th(IV) dissociation from bentonite colloids.

The percentages below refer to the total element concentration in the solution.
Figure 3.3.2 shows the removal of Th(IV) from solution for different Th/colloid pre-equilibration times.

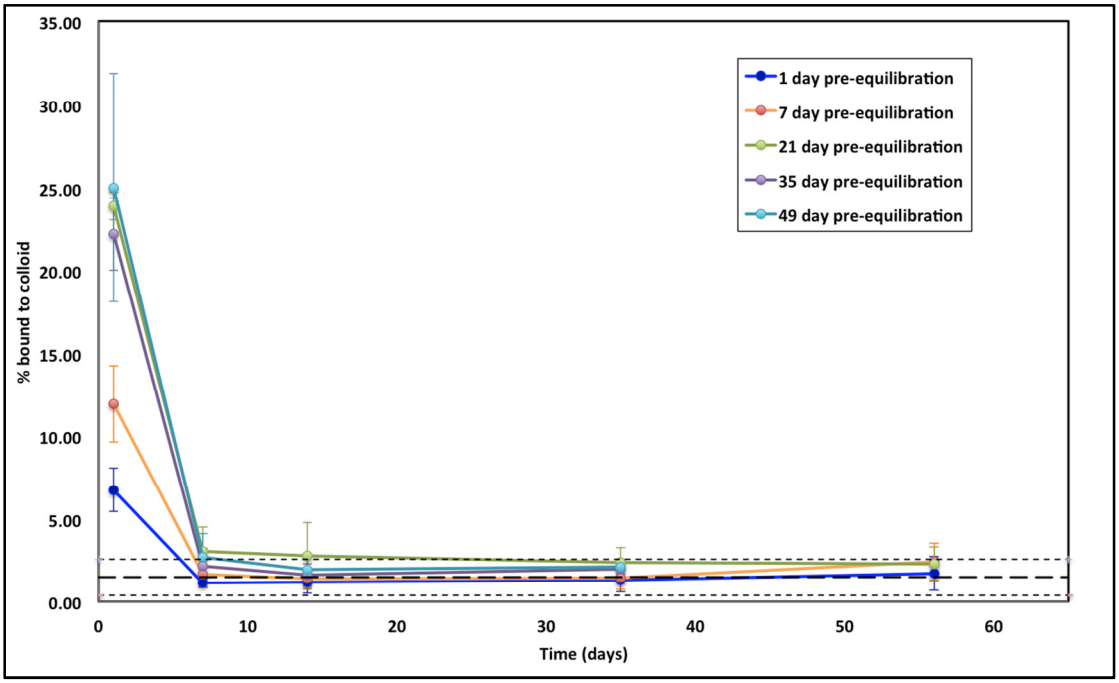

Figure 3.3.2. Plot of Th(IV) bound to bentonite colloids ([Th] = 3.79 x 10^{-12} M) vs time (days), (pH = 8.8 ± 0.2). The dashed black horizontal line represents the steady state distribution the dotted line above and below being the error range (1.5 ± 1.1 %)

The steady state position was determined in a separate experiment where Th was added to the Cellphos resin before the addition of bentonite colloid suspension. In that system, 1.5 ± 1.1 % of the Th remained in solution after 7 days equilibration, and this was taken to be the steady state position for the experiments shown in Figure 3.3.2 (the dashed horizontal line in Figure 3.3.2).
On initial contact, the Cellphos resin removes 76 – 93% of the Th from the solution. Analysis after 7 days of contact time shows 1.12 ± 0.26 %, 1.65 ± 0.82, 3.05 ± 1.48 % and 2.17 ± 1.04 % remaining associated with bentonite colloids for pre-equilibration times of 1, 7, 21 and 35 days respectively. Beyond this point, there is no significant difference between the different pre-equilibration times. However, before 7 days of contact with Cellphos, there is a difference, and for the first data point (1 day contact). The amount remaining in solution increases with increasing pre-equilibration time. Figure 3.3.3 shows the dissociation behaviour after 1 day of Cellphos contact for Th/bentonite colloid equilibration times of 1, 7, 21, 35 and 49 days.

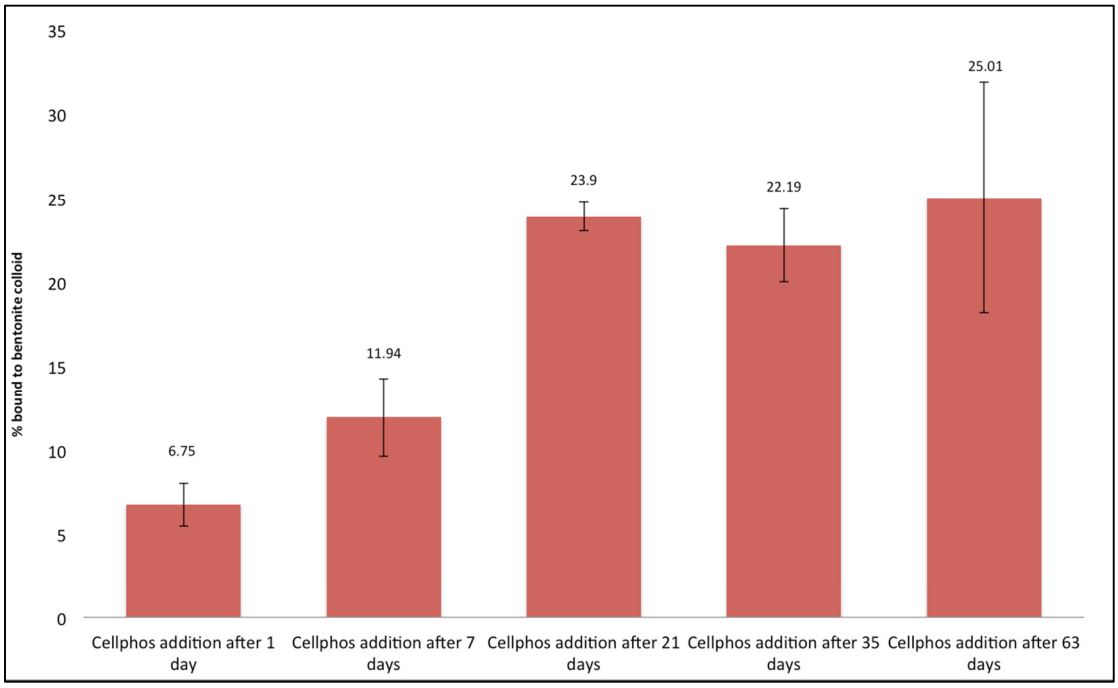

Figure 3.3.3, Th dissociation from bentonite colloids after 1 day contact with Cellphos for Th/bentonite colloid pre-equilibration times of 1, 7, 21, 35 and 63 days

6.75 % and 11.94 % of the Th is retained in solution after pre-equilibration times of 1 and 7 days, respectively. All subsequent pre-equilibration times (21, 35 and 63 days) retain approximately the same amount of Th (23.9, 22.2 and 25 %, respectively).
The data suggest that, following initial uptake on to the bentonite colloid, there is a slow change in speciation of the Th, which renders it less available. The dissociation data in Figures 3.3.2 and 3.3.3 show that this change appears to be complete within 21 days of pre-equilibration. The mechanism responsible for this behaviour is not clear. It seems likely that it is a ripening effect associated with a colloidal species.

Figure 3.3.2 shows that after 7 days contact with Cellphos, dissociation of Th from the bentonite colloids changes no further (i.e. no further dissociation is observed) for any sample points.
Bouby et al. (2011) performed batch desorption experiments with Th and bentonite colloids using humic acid as a competitor, over a period of 3 years. Some Th remained on the bentonite colloids (approximately 30 %), and this partial irreversibility was attributed to possible Th precipitation on the surface of colloids. In the studies described here, however, desorption of the Th from the bentonite colloids falls to within error of the steady state position within 7 days of contact time with the Cellphos resin, for all samples. In this system, there is no indication of irreversible binding to bentonite colloids.

^{241}Am(III) dissociation from bentonite colloids

The percentages given below are all relative to the total amount of element added to the systems.
Figure 3.3.4 shows the dissociation of Am(III) from bentonite colloids as a function of Am/colloid pre-equilibration time.

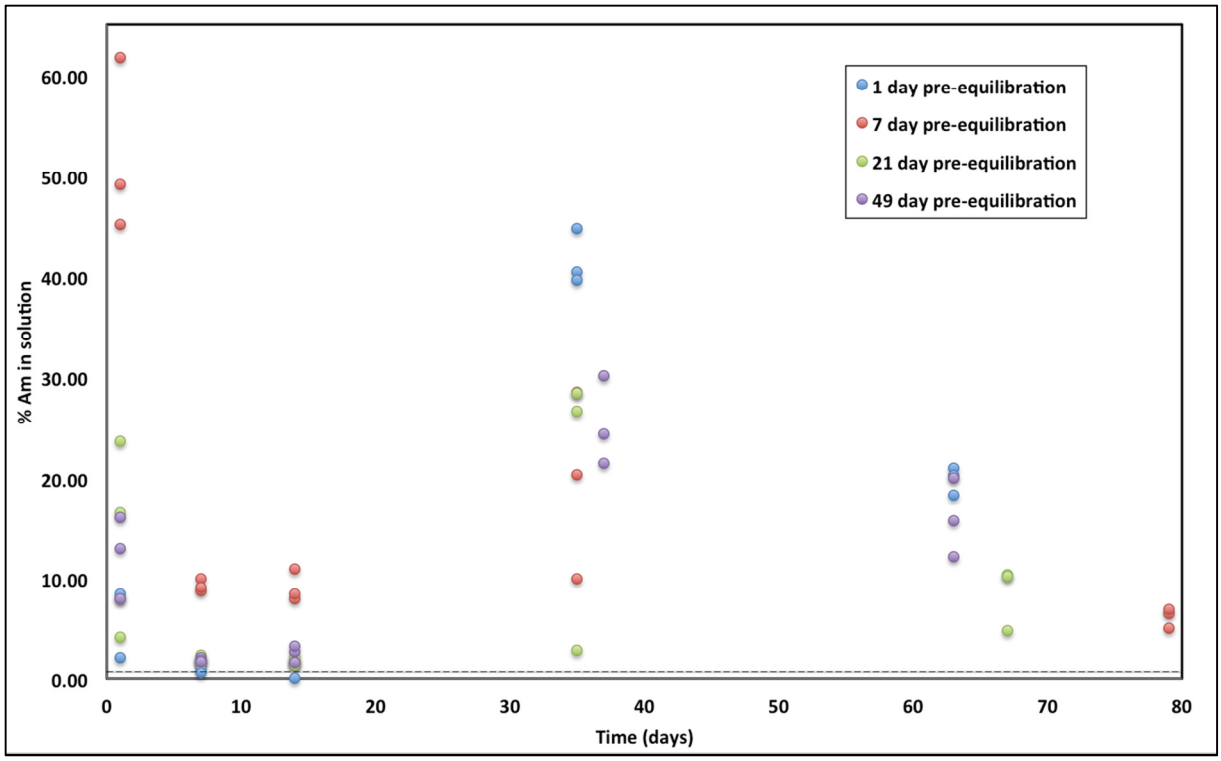

Figure 3.3.4. Dissociation plot of Am ([Am] = 3.27 x 10^{-9} M)) for different pre-equilibration times, as a function of Cellphos contact time (pH = 8.8 ± 0.2). Individual data points are shown to allow easier interpretation as there is relatively large scatter for some samples. The dashed black horizontal line represents the steady state distribution and the dotted line above and below is the associated uncertainty (0.7 ± 0.1 %)

The steady state position was determined in a separate experiment where Am was added to the Cellphos resin before the addition of bentonite colloid suspension. In that system, 0.7 ± 0.1 % of the Am remained in solution after 7 days equilibration, and this was taken to be the steady state position for the experiments shown in Figure 3.3.4 (the dashed horizontal line in Figure 3.3.4).

On initial contact, the Cellphos resin removes 50 - 94 % of the Am from the solution. Analysis after 7 days of contact time shows 1.23 ± 1.54 %, 9.31 ± 1.28, 1.95 ± 1.04 % and 1.94 ± 0.46 % Am remaining in solution for pre-equilibration times of 1, 7, 21 and 49 days, respectively. From day 35 of the experiment, there is a change in the behaviour, with a portion of Am being released from the Cellphos (41.6 ± 5.6 %, 19.6 ± 18.6 %, 19.3 ± 33.62 % and 25.4 % ± 8.8 % for pre-equilibration times of 1, 7, 21 and 49 days, respectively).

This release of Am by Cellphos was unexpected, since preliminary experiments with Am and Cellphos showed no such behaviour, but these were only performed over a 7 day period, while Figure 3.3.4 shows that this behaviour is not observed until after 14 days. However, within 70 days of Cellphos contact, the Am has been removed from the solution again.

It is clear that the behaviour observed for Am is not the same as that in the Eu dissociation work in section 3.1. The Eu dissociation studies performed in section 3.1 used Dowex ion exchange resin, whereas the Am studies performed here used Cellphos. The only other differences in the experimental setups is the concentration of metal added. The experiments in Section 3.1 used [Eu] = 1.02 × 10^{-10} M, whilst these used [Am] = 3.27 × 10^{-9} M.

In both Eu and Am experiments, the pH remained unchanged, Cellphos is capable of binding metal ions below pH 5 (Padilha et al. 1997) and its optimum binding range is pH 4.0 to 9.0 (Li et al. 2002) so this experiment is within the pH range of this study.

ICP-AES analysis was performed for dissolved phosphate to assess whether the behaviour seen in the Am experiments arose from degradation of the Cellphos resin (data not shown), but no dissolved

phosphate was detectable, suggesting that degradation does not occur. Moreover, any degradation of Cellphos might reasonably be expected to lead to similar behaviour in the Th experiments, but that was not observed. Extended reviews of the literature on Cellphos as a chelating resin also showed no evidence of Cellphos degradation. It is likely that the Am does not behave as the Eu because, in these systems, their speciation is different.

Am radiocolloids have been observed in these types of experimental systems (Ijima et al. 2008; Ijima et al. 2010; Mori et al. 2003), and the size distribution of Am (Figure 3.3.1) suggests that intrinsic colloids or other polymeric complexes may form in the case of Am. In the Eu experiments (Section 3.1), no evidence of Eu radiocolloids was observed. Further, the speciation calculations (Tables 3.3.1 – 3.3.3) predict that the Am system is supersaturated with respect to amorphous phases, but the Eu system is not. Therefore, it seems likely that the difference in behaviour is due to the formation of amorphous hydroxide/carbonate phases that remain in solution as intrinsic colloidal material.

The differences between Am and Eu may be important. Association/dissociation experiments of this type often use Eu(III) as an analogue of Am(III), with the assumption that experimental observations for the Eu are directly transferrable to Am, because of their similar chemistries. The data from these studies suggest that the speciation of Am and Eu can be different in some circumstances and that the total concentration of the radionuclide may be critical.

3.4 Spectroscopic studies of neptunium sorption on corundum and montmorillonite

The authors involved in the work in this section are: O. Elo, N. Huittinen, K Müller (Helmholz-Zentrum Dresden-Rossendorf, Institute of Resource Ecology, P.O. Box 510119, D-01314, Dresden, Germany). P Hölttä (Laboratory of Radiochemistry, Department of Chemistry, P.O. Box 55, FIN-00014 University of Helsinki, Finland).

In these experiments, neptunium(V)-237 sorption on montmorillonite has been studied under simplified but environmentally relevant conditions. The aluminium oxide corundum (α-Al_2O_3) has been used as a model phase for the reactive aluminol groups on the montmorillonite surface. Batch sorption experiments were conducted to obtain valid information on the amount of neptunium sorption on the mineral surfaces even though very little knowledge on the chemical nature of the formed neptunium species can be extracted. Batch sorption experiments are reported in Deliverable D-N°:3.8: "Macroscale investigations on colloid mobility in near-natural systems". Detailed information on the complexation mechanism and coordination of neptunium to the mineral surfaces was obtained by Zeta potential measurements and Attenuated Total Reflection Fourier-transform Infrared (ATR FT-IR) spectroscopy. ATR FT-IR spectroscopy provides *in-situ* information on the sorption complexes based on the characteristic vibrational modes of sorbed molecule species.

3.4.1 Materials and Methods

The sodium montmorillonite used in this work has been isolated from Wyoming Volclay MX-80 bentonite and purified by B^+Tech Oy, Finland. The mineral was used as received in the batch sorption and spectroscopic investigations. Within this work the specific surface area of montmorillonite was determined by N_2-BET method. The specific surface area was found to be 49.6 g^2/cm. Corundum (α-Al_2O_3), aluminium oxide, was provided by Taimicron.

Neptunium(V) speciation

Zeta potential

Zeta potential measurements were conducted to provide information on surface charge and on the complexation mode i.e. whether Np(V) outer- or inner-sphere complexation occurs on the mineral surface. The measurements were conducted with Malvern Zetasizer Nano ZS for montmorillonite with and without Np(V). The Zeta potential measurements were conducted using a montmorillonite solid concentration of 0.25 g/l in 10 mM NaCl. The pH was adjusted with 1 – 0.01 M NaOH and HCl from 3 to 11 and all the measurements were carried out under N_2 atmosphere. Zeta potential measurements with neptunium were conducted at pH 7 – 11 where moderate to strong Np(V) sorption occurs.

ATR FT-IR measurements

Attenuated total reflection Fourier-transform infrared (ATR FT-IR) spectroscopy was applied for the molecular identification of Np(V) surface species on corundum and montmorillonite. Infrared spectra were measured from 1800 to 600 cm^{-1} on a Bruker Vertex 70/v vacuum spectrometer, equipped with a Mercury Cadmium Telluride (MCT) detector. The spectral resolution was 4 cm^{-1} and spectra were averaged over 256 scans. A horizontal diamond crystal with nine internal reflections (CURA SamplIR

II, Smiths Inc.) was used. Further details on the experimental ATR FT-IR setup are compiled in Müller (2012).
The performance of *in situ* sorption experiments requires a thin mineral film prepared directly on the surface of the ATR diamond crystal as stationary phase. This was accomplished by pipetting aliquots of corundum and montmorillonite suspensions on the crystal followed by drying with a gentle stream of N_2. This procedure was repeated until an average mass density of 0.2 mg/cm^2 was obtained on the crystal. The mineral film was conditioned by flushing with the blank solution (0.01 M NaCl, pH 10) for 60 min using flow cell (V = 200 µl) at the rate of 100 µl/min. Subsequently, the sorption reaction was induced by rinsing the stationary phase with the Np(V) solution (50 µM in 0.01 M NaCl at pH 10) for 120 min. Finally, the loaded mineral phase was flushed again with the blank solution (60 min) in order to gain more information on the reversibility of the sorbed Np(V) species. NaCl was used as a background electrolyte for the IR spectroscopic work because it shows no adsorption throughout the frequency range of interest in contrast to ClO_4^-.

RESULTS

Zeta potential

The surface charge and effect of pH on the surface charge can be determined by Zeta potential measurements. Data obtained for montmorillonite in the presence (red dots on figure 3.4.1) and absence (black squares on figure 3.4.1) of 10^{-6} M neptunium is seen in Figure . In the absence of neptunium, the surface charge of montmorillonite is negative over the whole investigated pH-range. Thus, no isoelectric point (IEP) could be assigned for the mineral. The lack of an IEP has been attributed to the constant negative surface charge of the planar surface sites. In the presence of neptunium, the montmorillonite surface potential is increased by approximately 15 mV. Decrease of Zeta potential in presence of neptunium indicates a change in surface charge, furthermore, possible inner-sphere complex.

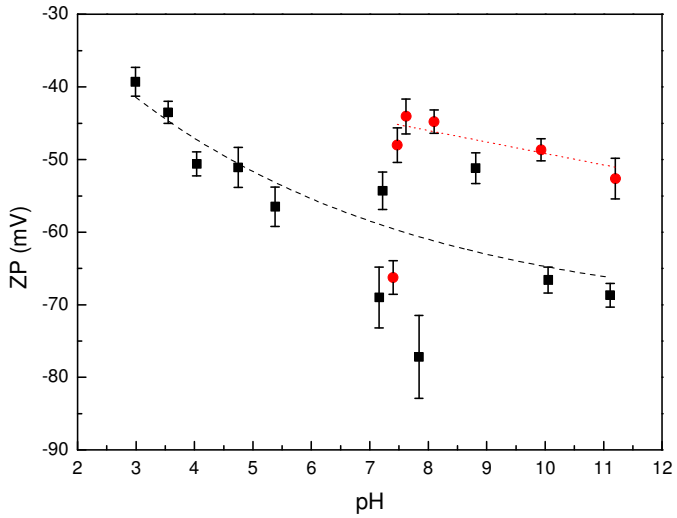

Figure 3.4.1. Zeta potential as a function of pH of 0.25 g/l montmorillonite in 10 mM NaCl solutions in the presence (red dots) and absence of neptunium (black squares).

ATR FT-IR spectroscopy

The course of an *in situ* Np(V) sorption experiment namely time-resolved infrared spectra obtained during conditioning, sorption and flushing steps onto corundum is illustrated in figure

3.4.2 (A). Furthermore, a single spectrum of Np(V) sorption obtained on montmorillonite after 60 min of contact time is presented in figure 3.4.2 (B). The "Conditioning" spectrum (figure 3.4.2 A red trace) shows no significant bands indicating a stable stationary phase of corundum which is indispensable for the detection of sorbed species during the following Np(V) sorption process. The "Sorption" spectra are shown in figure 3.4.2 A (black traces). These ATR FT-IR difference spectra are calculated between the conditioning and at several time steps after induction of Np(V) sorption. The progress of Np(V) accumulation on the corundum surface can be monitored on-line by the time-dependent increase of the adsorption band at 790 cm^{-1}. This peak is assigned to the antisymmetric stretching mode ν_3 of the sorbed NpO_2^+. The presence of one single band showing a constant frequency maximum and bandwidth throughout the sorption time of 120 min indicates the presence of only one type of surface species. After about 60 minutes, the intensity increase was considerably reduced indicating that an equilibrium state at the interface was reached.

For the fully hydrated NpO_2^+ present in aqueous solution the ν_3 mode is observed at 820 cm^{-1}, serves as a reference for the investigation of Np(V) complexation reactions (figure 3.4.2 green line). Coordination of aqueous NpO_2^+ ions on surfaces generally reduces the force constants of the O=Np=O bonds. Thus, a displacement of water molecules from the first shell lowers the frequency of the ν_3 (NpO_2^+) stretching mode. The extent of this shift is found to be correlated with the type of surface coordination. Whereas chemical bonding, namely the formation of inner-sphere complexes results in a considerable red-shift, physical interaction, i.e. outer-sphere complexation, reveals only very small shifts because of the remaining intact first hydration sphere (Lefevre 2004, Müller 2009). A comparison of the data sets from corundum and montmorillonite (figure 3.4.2) and from former investigations of Fe_2O_3 and TiO_2 (Müller 2009, Gückel 2013) demonstrates that the frequency of the ν_3 of the sorbed Np(V) species is observed at ~790 cm^{-1} irrespective of the sorbing surface. The extent of the redshift of ~30 cm^{-1} upon sorption of the Np(V) ion on these mineral oxide surfaces suggests a similar type of surface complexation that is an inner-sphere surface complex.

Subsequent to sorption, "Flushing" of the corundum film with blank solution was performed in order to potentially provide information on the surface species, which can be easily removed. The difference spectra in figure 3.4.2 A (upper blue traces) were calculated from the spectra recorded at the end of the sorption step and after different time steps of flushing. In contrast to the sorption data, negative peaks showing significantly reduced intensities are observed between 1200 and 900 cm^{-1} and at 790 cm^{-1}. Hence, the spectral data indicates that a certain amount of the sorbed Np(V) complex is released from the mineral film in accordance to our desorption investigations presented above. This very high reversibility was not observed by Gückel et al. 2013, for neptunium adsorbed on the aluminum hydroxide gibbsite. Thus, sorption onto aluminol groups cannot be the explanation for the fast desorption kinetics. However, some similarities between the surface complexes on corundum and montmorillonite have to exist that differs from the neptunium complexes formed on the gibbsite surface.

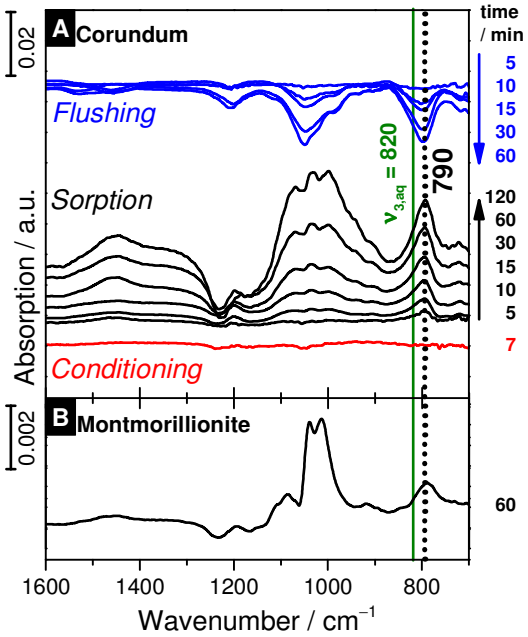

Figure 3.4.2. In situ time-resolved ATR FT-IR spectra of Np(V) sorption on corundum (A) and montmorillonite (B). (50µM Np(V), D_2O, 0.01 M NaCl, N_2, ~0.2 mg mineral cm^{-2}). For corundum the spectra of the conditioning, sorption and flushing process are shown at different times given (from bottom to top). For montmorillonite, only the spectrum obtained after 60 min of sorption is shown. Indicated values are in cm^{-1}.

3.5 Cd Interactions with Bentonite

The authors involved in the work in this section are: U. Alonso and T. Missana (CIEMAT).

Colloid contribution to radionuclide (RN) transport is subjected to the joint compliance of several conditions (Miller et al., 1994), including colloid existence, stability and mobility. The radionuclide / colloid bond irreversibility is also a fundamental condition to be verified. Within BELBAR project, CIEMAT is analysing each of the above mentioned aspects. In particular, the irreversibility of radionuclide sorption to bentonite colloids is being analysed both under dynamic and static conditions.
Previous radionuclide - colloid transport studies carried out under dynamic conditions in granite fractures indicated that radionuclide recovery is, in many cases, lower than expected considering the initial radionuclide - colloid association (Albarran et al., 2011; Missana et al., 2008a). The results on Cs transport and its reversibility behaviour during transport in presence of bentonite colloids in two granite fractures from Grimsel (Switzerland) and Aspö (Sweden) underground laboratories were presented in BELBAR Deliverable D3.3.
At present, the reversibility of radionuclide sorption to bentonite is being analysed under static conditions. To evaluate the extent of sorption reversibility, the kinetics of the sorption and desorption processes was analysed. Desorption can be promoted by chemistry changes (Missana et al., 2004) or by the presence of a third phase (Bouby et al., 2011; Bryan et al, 2012).
In the study presented in this Deliverable, desorption process was promoted by an increase in ionic strength. Cadmium was selected as bivalent heavy metal, with low fission product yield, for which little sorption data onto bentonite was available.

3.5.1 Materials and Methods

The bentonite used (FEBEX bentonite) comes from the Cortijo de Archidona deposit (Almeria, Spain) with high smectite content (93%) (Huertas et al., 2000). The cation exchange capacity (CEC) of the FEBEX clay is 102 ± 4 meq/100g. For sorption/desorption experiments, bentonite was conditioned in Na- homoionic with $NaClO_4$ as described in (Missana et al., 2008b).

Desorption studies
Studies were carried out with a ^{109}Cd solution in 0.1 M HCl that contained 37·MBq/mL and 500 ug Cd/mL $CdCl_2$ carrier. ^{109}Cd has a half-life of 462.6 days and decays by electron capture with a major gamma emission at 88 KeV. Experiments were carried out to a final Cd concentration of $1 \cdot 10^{-5}$ M, adding $CdCl_2$ (Merck).
The *kinetics of the sorption process* was analysed with 0.5 g/L bentonite suspension conditioned in $NaClO_4$ $1 \cdot 10^{-2}$ M at three different pH (4, 7 and 10), with an initial cadmiun concentration of 10^{-5} M. All experiments were carried out in polystyrene tubes (10 mL) under atmospheric conditions.
For each selected pH, five equal samples were prepared. The tubes were maintained in continuous stirring during selected equilibrium times (1 day, 15 days and 30 days). After this time, one of the samples of each pH set was centrifuged (21500g during 30 min). After the solid separation, three aliquots of the supernatant were extracted from each tube for the analysis of the Cd final activity in solution (C_f). Cd activity was measured by gamma counting (Cobra Autogamma, Packard). Cd concentration adsorbed on bentonite was determined by subtraction to the initial Cd concentration (10^{-5} M and distribution coefficients (Kd) were determined as described in (Missana et al., 2004). The amount of Cd adsorbed onto the centrifuge tubes was always checked.
To analyse the *kinetics of desorption process,* kinetic contact times are considered as pre-equilibrium times (1, 15 or 30 days). Once selected kinetic contact time elapsed, $NaClO_4$ was added to the four remaining samples of each pH set, to increase ionic strength from 10^{-2} M to 10^{-1} M. After ionic

strength increase, each set of samples was also maintained in continuous stirring during selected desorption times (1, 7, 15 and 30 days. Afterwards, samples were centrifuged, and Cd concentration in solution was determined as previously described for sorption experiments. To analyse the desorption behaviour, measured Cd concentration values will be compared to those previously measured at lower ionic strength.
Cd sorption edges at different pH (3 to 11) and ionic strengths ($5 \cdot 10^{-4}$ to 10^{-1} M) and sorption isotherms varying the radionuclide concentration (were also carried out to describe Cd sorption onto bentonite by surface complexation modelling (Missana e*t al*, 2015).

Results

The Cd stability constants and speciation was verified (Powell et al., 2011; Zirino and Yamamoto, 1972)and the selected Cd database is reported in (Alonso et al., 2015). Considering the presence of Cl[-] and HCO_3[-] as organic ligands, Cd^{2+} is the dominant aqueous specie up to pH 8 with and around 5% presence of $CdCl^+$. The hydrolysed species $CdOH^+$ starts playing a relevant role for pH higher than 8.
Figure 3.5.1 shows the Cd distribution coefficients measured, as a function of time, on bentonite suspended in $NaClO_4$ 0.01 M at three different pH conditions. At pH 4 and 7 the Kd measured after 1 day of contact remained constant up to 30 days, but at pH 10 sorption slightly increases over time.

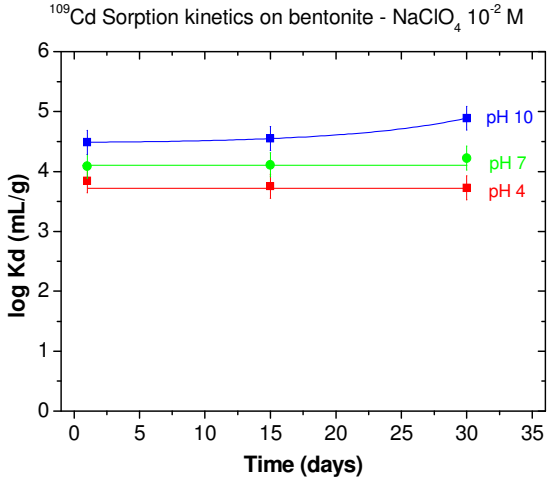

Figure 3.5.1. Cadmiun sorption kinetics onto bentonite in $NaClO_4$ 0.01 M at three different pH.

After different sorption pre-equilibrium times at 10^{-2} M, the ionic strength was increased to 10^{-1} M to analyse the desorption kinetics .The cadmiun concentration (M) measured in the liquid phase (M) as a function of time after increasing ionic strength to 10^{-1} M is presented in Figure 3.5.2, for the three studied pH: 4, 7 and 10. In the Figure, the time scale of desorption experiments is presented considering the initial pre-equilibrium time at the lower ionic strength 10^{-2} M (1, 15 or 30 days).
At pH 4 and 7, Cd concentration in the liquid phase increases after 1 day, and values are constant upon time, indicating Cd is reversible. At those pHs, Cd sorption on bentonite is expected to occur by cation exchange (Missana *et al.*, 2015) so that a decrease in sorption (concentration increase in the liquid phase) by increasing ionic strength is expected. The obtain values decreasing ionic strength at fully comparable to those measured at 10^{-1} M (Missana *et al.*, 2015). Considering that no- kinetics is observed in any case, Cd sorption on bentonite for pH 4 and 7 can be considered reversible. Indeed, it is generally assumed that cation exchange process is fast and reversible (Stumm, 1992), showing the same sorption and desorption rates. Cadmium reversibility from other clays was observed (Comans, 1987). To calculate Cd dissociation constants, shorter experiments should be carried out because at pH 4 and 7, both sorption and desorption are complete after one day.

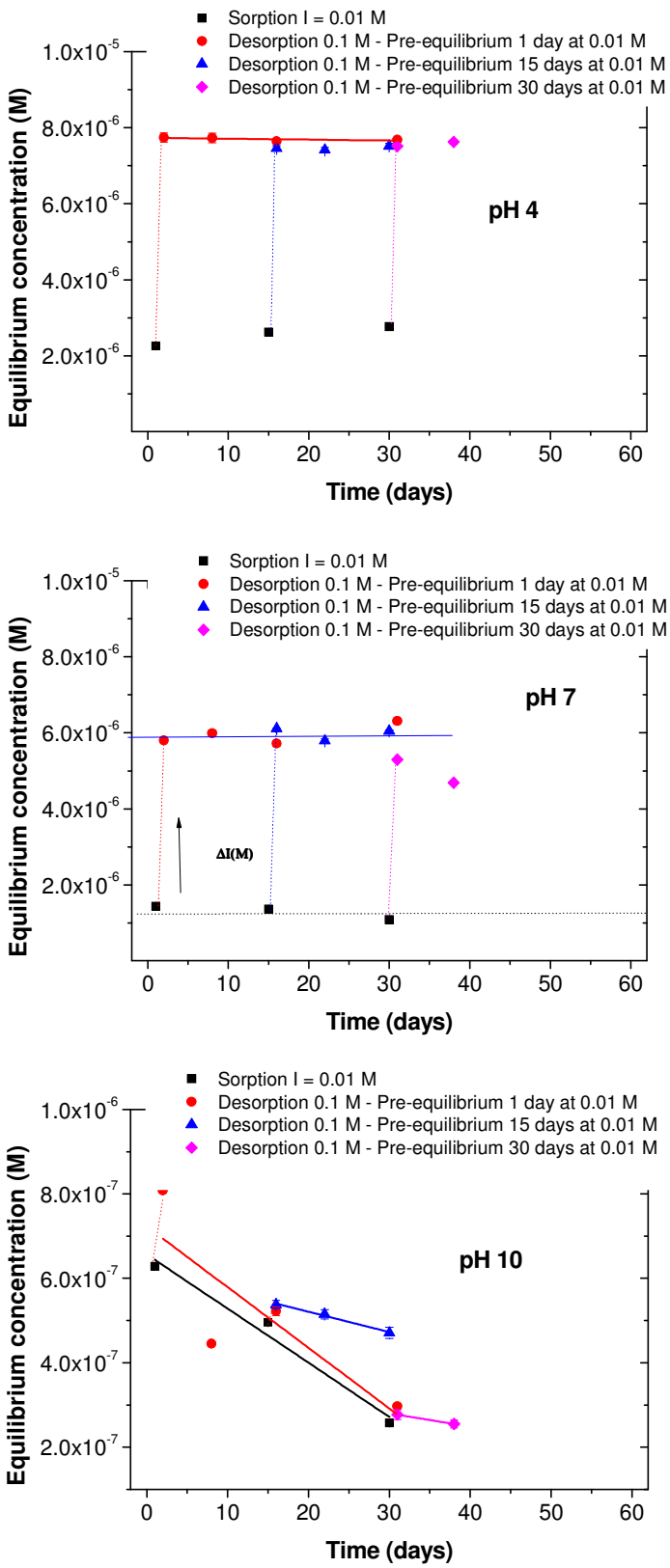

Figure 3.5.2. Cadmiun concentration (M) measured in the liquid phase (M) as a function of time after increasing ionic strength to 10^{-1} M to promote desorption at three different pH: 4, 7 and 10. The time scale of desorption experiments is presented considering the initial pre-equilibrium time at lower ionic strength 10^{-2} M (1, 15 or 30 days).

However, the Cd desorption at pH 10 presents much complex behaviour than in the above mentioned cases (figure 3.5.2). At pH 10, Cd sorption is expected to take place by surface complexation (Missana *et al.*, 2015) and Cd sorption increased over time (figure 3.5.1). Kinetics of desorption experiments showed a dependence on initial pre-equilibrium time, which suggests that Cd is not reversible, under these conditions.

3.6 Analysis of uranium, neptunium, plutonium, amercium and curium isotopes below PPQ levels in samples from deep geological repositories

The authors involved in the work in this section are: F. Quinto, M. Lagos, M. Plaschke, T. Schafer, H. Geckeis (Institute for nuclear waste disposal (INE), Karlsruhe institute of technology, Hermann-von-Helmholtz-Platz 1 76344 Eggenstein Leopoldshafen) and P. Steier (*VERA Laboratory, Faculty of Physics, University of Vienna, Währinger Straße 17, A-1090 Vienna, Austria)*

This contribution has been published as:
Quinto, Golser, Lagos, Plaschke, Schäfer, Steier, Geckeis 2015: Accelerator Mass Spectrometry of Actinides in Ground- and Seawater: An Innovative Method Allowing for the Simultaneous Analysis of U, Np, Pu, Am, and Cm Isotopes below ppq Levels. *Analytical Chemistry*, 87(11), 5766-5773.

Accelerator Mass Spectrometry (AMS) is presently one of the most sensitive analytical techniques for the determination of actinides; that is due to the stripping process and acceleration of the ions to MeV energies providing both the destruction of molecular isobaric background and a strong reduction of tailing interferences. The Vienna Environmental Research Accelerator (VERA) has developed abundance sensitivities (AS) for ^{236}U, ^{237}Np and ^{239}Pu relative to ^{238}U at levels $\leq 10^{-15}$ (Steier et al. 2014) and detection limits (DL) at the value of 10^4 atoms per sample (Steier et al. 2010). These features allow accurate measurements of actinide concentrations below ppq levels, particularly advantageous when a limited sample size is available. Such an analytical challenge is encountered, e.g., when investigating environmental samples affected by low levels nuclear contamination, like the global fallout, or in the frame of field experiments employing actinide tracers, like the Colloid Formation and Migration Project (CFM) at the Grimsel Test Site.
A further challenge in the determination of ^{237}Np and of ^{243}Am lies in the non-availability of pure enough isotopic tracers for mass spectrometric measurements when investigating concentrations of 10^5 to 10^8 atoms in a sample. To overcome this limitation, at INE we have investigated the use of non-isotopic tracers, developing a new method in which different actinide nuclides can be measured sequentially without previous chemical separation from each other exploiting the exceptional AS of AMS. The chemical treatment consists principally in the purification of the group of the actinides from the matrix elements with a $Fe(OH)_3$ co-precipitation.
Multi-isotope solutions obtained with known amounts of ^{233}U, ^{237}Np, ^{239}Pu, ^{243}Am and ^{248}Cm in groundwater samples were submitted to the same chemical treatment of the samples with corresponding matrix. Such “calibration samples” were repeatedly measured together with the investigated samples in order to compensate for the different chemical and ionization yields of the several actinides in the Cs negative ions sputtering source of AMS.
This procedure, allowing for the first time the simultaneous mass spectrometric determination of ultra-trace levels of several actinide nuclides in presence of naturally occurring U, is especially suited to groundwater and seawater samples. At the Grimsel Test Site, in the frame of the CFM Project, a first radionuclide tracer test under low-flow conditions has been performed in 2012 (run 12-02). In this experiment ^{237}Np, ^{242}Pu and ^{243}Am have been injected in water conducting granodiorite fractures in order to investigate the colloid mediated transport of the actinides.
In the present study we have investigated six groundwater background (BG) samples, which were collected in the tailing of the tracer pulse experiment breakthrough curve from 60 up to 210 days after the start of the experiment. The concentration of the injected tracers in these samples was supposed to be below the detection limits of HR ICP-MS, employed for the measurements of the preceding samples, and equal to 10 ppq.

The size of the BG samples was limited to a mass of 500 g or to 250 g, in which the concentrations of ^{237}Np and ^{242}Pu have been determined by using ^{239}Pu as yield tracer, while that of ^{243}Am by using ^{248}Cm.

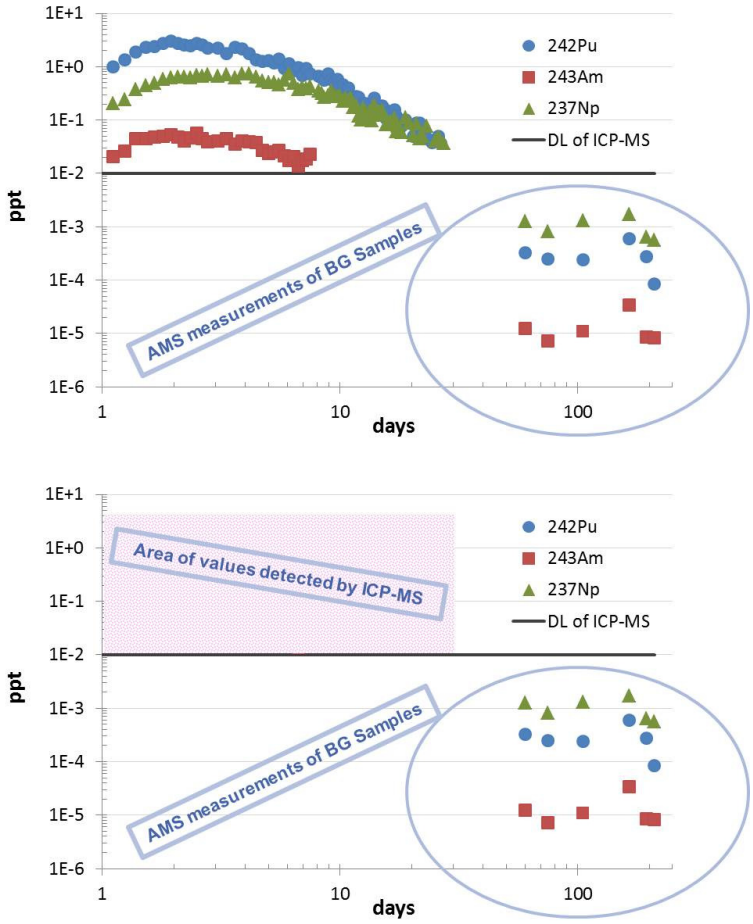

Figure 3.6.1: (a) ^{242}Pu (blue circles), ^{237}Np (green triangles) and ^{243}Am (red squares) concentrations in the eluent fractions of the experiment run 12-02 in the frame of the CFM Project. Above and below the black line indicating the DL of HR ICP-MS, the area of data detectable with the first technique and the data obtained with AMS, respectively, are depicted.

The detection of ^{237}Np, ^{242}Pu and ^{243}Am down to the levels of fg/g and ag/g was successful in the investigated samples, as shown in Fig. 1. The use of non-isotopic tracers has led to a higher uncertainty in the determination of ^{237}Np and ^{243}Am than of ^{242}Pu. In fact, while, the maximum relative uncertainty on the measured values of ^{239}Pu, due solely to the counting error, is equal to ~ 5%, the relative uncertainties of the measured values of ^{237}Np and ^{243}Am reach respectively ~ 16% and ~ 24%. However it is possible to observe for every investigated isotope a trend of concentration leading to a maximum in the sample corresponding to the sampling time of 165 days, as shown in Fig 3.6.1. These findings prove that the long term release and retention of actinide tracers can be studied in samples collected up to 6 months after the starting of the experiment.
The extraordinary sensitivity of AMS, allowing the detection of ultra-trace levels of actinides, provides the capability to observe their behaviour in a variety of environmental systems. We exploit this feature in field studies whose results are complementary to those of the fundamental research on the speciation of actinides.

4 Conclusions and Implications

4.1 Conclusions of europium studies (section 3.1)

No evidence for 'irreversible' binding of Eu by bentonite has been observed. Eu(III) does bind to bulk bentonite and bentonite colloids and there was both a fast and slow dissociation, but there was no sign that the radionuclides were bound permanently.

For bulk bentonite, beyond approximately 100 days pre-equilibration time, the amount of Eu in the most slowly dissociating fraction was effectively constant. However, the experiments suggested that there is a change in dissociation behaviour over pre-equilibration times up to 1 week, with a reduction in the slowest dissociation rate constant of approximately an order of magnitude. In addition to a significant fraction that dissociates instantaneously and some material with intermediate rates, there does seem to be a most slowly dissociating fraction that has a characteristic rate constant of approximately 4.3×10^{-8} s^{-1}.

There was a difference between the colloid and bulk dissociation. The first order rate constant was significantly higher (i.e. faster reaction rate) for colloids, with an average dissociation rate constant of 8.8×10^{-7} s^{-1}, over an order of magnitude faster than for bulk bentonite. There was also only a single rate constant in the colloid system, and the amount slowly dissociating did not increase beyond a pre-equilibration time of one day. Previous work with humic substances has shown that in a system where some portion of colloid associated radionuclides dissociate slowly, this will dominate transport (Bryan et al. 2007). Whether or not the rate constants measured here mean that colloidal transport is significant will depend upon transport residence times in the subsurface.

4.2 Conclusions of uranium studies (section 3.2)

Because ^{232}U(VI) was used in the dissociation experiments, it only gave a small window of time to perform the experiments (approximately 65 days) before the in-growth of ^{228}Th started to affect the data, and therefore the experiments did not reach steady state. However, all systems were tending towards the equilibrium position, and as such, there is no evidence that the U(VI) in this study was bound to the bentonite colloids permanently (irreversibly).

It is clear that the association to bentonite colloids is smaller for U(VI) compared to Eu(III) (this study suggests approximately 54 ± 1.2 %, with Eu(III) it is approximately 100 %). Of the 54 % of U(VI) that is colloid bound, approximately 30 % dissociates over a 4 day period and 24% dissociates slowly.

Previous studies have shown that a very small percentage of the U interacting with bentonite colloids (Mori et al. 2003, Bouby et al. 2010, etc.). This study useda much smaller concentration of U (two to three orders of magnitude less) and a much higher concentration of bentonite colloids (approximately 9 times more). Therefore, it is possible that the previous studies reached a saturation limit with the colloids that was not observed in this study. Speciation modelling suggests that carbonate complexation may compete with binding to the bentonite.

Even though the trivalent Eu shows an apparently stronger affinity for bentonite colloids than U(VI), the dissociation rate constants are very similar. At least for these two ions, it seems that the chemistry of the metal ion has little effect on the dissociation rate constant for the most slowly dissociating fraction. There does seem to be minor differences in dissociation at short times, but for the most important fraction, the behaviour is comparable.

These experiments have provided a measured value for the first order dissociation rate constant for uranyl dissociating from bentonite colloids ($(5.6 \pm 4.2) \times 10^{-7}$ s^{-1}). When combined with other data, principally migration rate, this result will allow the significance of bentonite colloid transport of U to be assessed.

4.3 Conclusions of thorium and amercium studies (section 3.3)

Thermodynamic speciation modelling shows that in these systems, at this pH (8.8), even with very low concentrations ([Th] = 3.79×10^{-12}M; [Am] = 3.29×10^{-9}M) that super-saturation of certain phases can still occur. This can have an effect on the behaviour of . For both Th and Am, it is likely that significant fractions are present as intrinsic colloid or polymeric species.

Approximately 78% of the Th(IV) is found in the > 200 nm size fraction. However, this material dissociates relatively quickly, although there is some evidence for the ripening of the Th(IV) solution loading with time associated with an increasing resistance to dissociation. Virtually all of the Th is removed from solution within 7 days. Mori et al (2003) found slower dissociation of Th, which they speculated was due to a Th(IV) surface precipitate. However, these studies used a much higher Th(IV) concentration, and it is possible that explains the difference.

Am(III) shows limited association with the bentonite colloids in these systems (at most 20 %), which may arise from the formation of Am intrinsic colloids, as observed in previous studies (Ijima et al. 2008; Ijima et al. 2010; Mori et al. 2003). Speciation modelling shows that there are Am(III) phases predicted to be supersaturated in this system, which could explain the poor binding affinity of Am(III) to bentonite colloids in this system.

4.4 Conclusions of neptunium spectroscopic studies (section 3.4)

Np(V) sorption onto corundum and montmorillonite was investigated by batch sorption and desorption studies, Zeta potential measurements and ATR FT-IR spectroscopy were used to obtain information of Np(V) coordination, bond lengths and reversibility. Np(V) sorption on corundum and montmorillonite increased in the alkaline pH-range, and for montmorillonite a constant 10 % sorption was found. The negatively charged planar sites of montmorillonite adsorbed neptunium in the acidic pH range, causing the constant sorption. Ion exchange was not expected or observed for corundum, because of its high IEP. The high reversibility for both minerals was also apparent in the IR studies. ATR FT-IR spectroscopy results indicated an inner-sphere complex on both minerals. The obtained results from the Zeta potential measurements supports the assumption of an inner-sphere complex made based on the ATR FT-IR spectroscopy. In situ ATR FT-IR spectroscopy using a flow cell, applied the first time to montmorillonite in this study, is an applicable method for the detection of very low absorption changes in front of a strong absorbing background.

4.5 Conclusions of cadmium (section 3.5)

The kinetics of Cd sorption and desorption onto bentonite colloids was analysed in $NaClO_4$ at different pH conditions. Desorption was promoted by an increase in ionic strength. The results showed that in the areas where Cd is sorbed by cationic exchange process, Cd binding is fully reversible, while under alkaline conditions, where surface complexation dominates, Cd seems to be irreversibly sorbed.

For next studies, the irreversibility of other radionuclides will be analysed as well under batch experiments. Moreover, the reversibility of radionuclide-colloid binding will be also analysed under dynamic conditions in granite fractures, to compare radionuclide-colloid dissociation under both static and dynamic conditions, incorporating the granite phase.

4.6 Conclusions of accelerator mass spectrometry analysis (section 3.6)

The findings in this section prove that the long term release and retention of actinide tracers can be studied in samples collected up to 6 months after the starting of the experiment.
The extraordinary sensitivity of AMS, allowing the detection of ultra-trace levels of actinides, provides the capability to observe their behaviour in a variety of environmental systems. This feature is exploited in field studies whose results are complementary to those of the fundamental research on the speciation of actinides.

Acknowledgements

The authors would like to thank all of those that have contributed to the experimental work in this report and the European Union for funding this work through the BELBaR project.

References

N. Albarran, T. Missana, M. Garcia-Gutierrez, U. Alonso, M. Mingarro, 2011. Journal of Contaminant Hydrology, 122, 2011, 76-85.

U. Alonso, N. Mayordomo, and T. Missana, (2015). Cadmium adsorption onto alumina nanoparticles for their use in geochemical barrier for contaminant migration. *CIEMAT publication , Madrid (Spain). In press.*

M. Bouby, A. Filby, H. Geckeis, F. Geyer, R. Götz, W. Hauser, F. Huber, S. Keesmann, B. Kienzler, P. Kunze, M. Küntzel, J. Lützenkirchen, U. Noseck, P. Panak, M. Plaschke, A. Pudewills, T. Schäfer, H. Seher, C. Walther, 2010A, Sorption reversibility studies: Comparison of fracture filling material (FFM) from Grimsel (Switzerland) and Äspö (Sweden) in *Colloid/Nanoparticle formation and mobility in the context of deep geological nuclear waste disposal (Project KOLLORADO-1; Final report),* Thorsten Schäfer & Ulrich Noseck (Eds.), FZKA Wissenschaftliche Berichte, FZKA 7515, pg 25 - 36.

M. Bouby, A. Filby, H. Geckeis, F. Geyer, R. Götz, W. Hauser, F. Huber, S. Keesmann, B. Kienzler, P. Kunze, M. Küntzel, J. Lützenkirchen, U. Noseck, P. Panak, M. Plaschke, A. Pudewills, T. Schäfer, H. Seher, C. Walther, 2010B, Core migration studies in *Colloid/Nanoparticle formation and mobility in the context of deep geological nuclear waste disposal (Project KOLLORADO-1; Final report),* Thorsten Schäfer & Ulrich Noseck (Eds.), FZKA Wissenschaftliche Berichte, FZKA 7515, pg 25 - 36.

M. Bouby, A. Filby, H. Geckeis, F. Geyer, R. Götz, W. Hauser, F. Huber, S. Keesmann, B. Kienzler, P. Kunze, M. Küntzel, J. Lützenkirchen, U. Noseck, P. Panak, M. Plaschke, A. Pudewills, T. Schäfer, H. Seher, C. Walther, 2010C, *Colloid/Nanoparticle formation and mobility in the context of deep geological nuclear waste disposal (Project KOLLORADO-1; Final report),* Thorsten Schäfer & Ulrich Noseck (Eds.), FZKA Wissenschaftliche Berichte, FZKA 751.

M. Bouby, H. Geckeis, J. Lutzenkirchen, S. Mihai, T. Schafer, 2011, Interaction of bentonite colloids with Cs, Eu, Th and U in presence of humic acid: A flow field-flow fractionation study, Geochimica et Cosmochimica Acta, 75, 3866–3880.

M.H. Bradbury, B. Baeyens, H. Geckeis, T. Rabung, 2005, Sorption of Eu(III)/Cm(III) on Ca-montmorillonite and Na-illite. Part 2: Surface complexation modelling, Geochimica et Cosmochimica Acta, 69, 5403–5412.

M.H. Bradbury B. Baeyens, 1999, Modelling the sorption of Zn and Ni on Ca-montmorillonite, Geochimica et Cosmochimica Acta, 63, 325–336.

M.H. Bradbury B. Baeyens, 2006, Modelling sorption data for the actinides Am(III), Np(V) and Pa(V) on montmorillonite Radiochim. Acta, 94, 619–625.

N.D. Bryan, D.L.M. Jones, R.E. Keepax, D.H. Farrelly, L.G. Abrahamsen, P. Warwick, N. Evans, 2007, The Role of Humic Non-Exchangeable Binding in the Promotion of Metal Ion Transport in the Environment, Journal of Environmental Monitoring, 9, 329-347.

N.D. Bryan, L. Abrahamsen, N. Evans, P. Warwick, G. Buckau, L.P. Weng and W.H. Van Riemsdijk, 2012, The effects of humic substances on the transport of radionuclides: Recent improvements in the prediction of behaviour and the understanding of mechanisms. Applied Geochemistry, 27, 378-389.

R.N.J. Comans, 1987, Adsorption, desorption and isotopic exchange of cadmium on illite: evidence for complete reversibility. Water Research, 21, 1573–1576.

R.N.J. Comans, M. Haller, P. Depreter, 1991, Sorption of cesium on illite – nonequilibrium behavior and reversibility. Geochimica Cosmochimica Acta, 55, 433–
440.

A. de Koning, R.N.J. Comans, 2004, Reversibility of radiocaesium sorption on illite. Geochimica Cosmochimica Acta, 68, 2815–2823.

A. Delos, C.Walther, T. Schaefer and S. Buechner, 2008, Size dispersion and colloid mediated radionuclide transport in a synthetic porous media. Journal of Colloid and Interface Science, 324, 212-215.

L. Duro, E. Cera, M. Grive, C. Domenech, X. Gaona & J. Bruno. (2006) Development of the thermochimie thermodynamic database. Janvier. Andra report C. RP. 0ENQ. 06. 0001. P373.

C. Ekberg, Y. Albinsson, M. J. Comarmond & P. L. Brown (1999) Studies on the complexation behaviour of thorium(IV). 1. Hydrolysis equilibria, J. Solution Chem, 29, 1, 2000.

H. Geckeis, T. Schäfer, W. Hauser, T. Rabung, T. Missana, C. Degueldre, A. Möri, J. Eikenberg, T. Fierz, W.R. Alexander, 2004, Results of the Colloid and Radionuclide Retention experiment (CRR) at the Grimsel Test Site (GTS), Switzerland -Impact of reaction kinetics and speciation on radionuclide migration. Radiochimica Acta. 92, 765-774.

M. Grive, O. Riba, V. Montoya & L. Duro (2010) Update of the thermochimie database: Reporting of new data selection 2010. June 2010.

K. Gückel, A. Rossberg, K. Müller, V. Brendler, G. Bernhard, H. Förstendorf (2013). Spectroscopic identification of binary and ternary surface complexes of Np(V) on gibbsite. *Environmental Science Technology,* **47**(24), pp. 14418-25.

Z. Guo, J. Xu, K. Shi, Y. Tang, W. Wu, Z. Tao, 2009, Eu(III) adsorption/desorption on Na-bentonite: Experimental and modeling studies. Colloids and Surfaces A: Physicochemical and Engineering Aspects, 339, 126–133.

W. Hauser, H. Geckeis, J.I. Kim, T. Fierz, 2002, A mobile laser-induced breakdown detection system and its application for the in situ-monitoring of colloid migration. Colloids and Surfaces A: Physicochemical and Engineering Aspects, 203, 37-45.

B.D. Honeyman, 1999, Colloidal culprits in contamination. Nature, 397, 23–24.

F. Huber, P. Kunze, H. Geckeis, T. Schäfer, 2011, Sorption reversibility kinetics in the ternary system radionuclide-bentonite colloids/nanoparticles-granite fracture filling material. Applied Geochemistry, 26, 2226–2237.

http://www.grimsel.com/gts-phase-vi/cfm-section.

K. Iijima, Y. Shoji & T. Tomura (2008) Sorption behaviour of americium on bentonite colloid. Radiochim. Acta, 96, 721-730.

K. Iijima, T. Tomura, M. Tobita and Y. Suzuki, 2010, Distribution of Cs and Am in the solution-bentonite colloids-granite ternary system: effect of addition order and sorption reversibility. Radiochimica Acta, 98, 729–736.

P. Ivanov, T. Griffiths, N.D. Bryan, G. Bozhikov and S. Dmitriev, 2012, The effect of humic acid on uranyl sorption onto bentonite at trace uranium levels. J. Environ. Monit., 14, 2968–2975.

P.Ivanov, T. Griffiths, N.D. Bryan, G. Bozhikov, S. Dmitriev, 2013, Interactions of $^{237}U/^{237}Pu$ with Bentonite, in Understanding of Radionuclide Colloid Interaction (with special emphasis on sorption reversibility), pages 10 – 14, Deliverable 3.3 BELBaR Project Report, Eds. N.Bryan and N. Sherriff.

A.A. Jennings and D.J. Kirkner, 1984, Instantaneous equilibrium approximation analysis. Journal of Hydraulic Engineering (A.S.C.E.), 110, 1700 – 1717.

O.Karnland, 2010, Chemical and mineralogical characterization of the bentonite buffer for the acceptance control procedure in a KBS-3 repository, SKB Technical Report, TR-10-60.

A. Kersting, D. Efurd, D. Finnegan, D. Rokop, J. Thompson, 1999, Migration of plutonium in the groundwater at the Nevada Test Site, Nature, 397, 56–59.

S.J. King, P. Warwick, A. Hall, N.D. Bryan, 2001, The dissociation kinetics of dissolved metal-humic complexes. Physical Chemistry Chemical Physics, 3, 2080-2085.

D. Koch, 2008, European bentonites as an alternative to MX-80, Science & Technology series no 334.

A. Kowal - Fouchard, R. Drot, E. Simoni , J. Ehrhardt, 2004, Use of Spectroscopic Techniques for Uranium(VI)/ Montmorillonite Interaction Modeling. Environmental Science and Technology, 38, 1399-1407.

P. Kunze, H. Seher, W. Hauser, P.J. Panak, H. Geckeis, Th. Fanghänel, T. Schäfer, 2008, The influence of colloid formation in a granite groundwater bentonite porewater mixing zone on radionuclide speciation. Journal of Contaminant Hydrology, 102, 263–272.

M. Laaksoharju, S. Wold, 2005, The colloid investigations conducted at the Aspo Hard Rock Laboratory during 2000 – 2004, SKB Technical Report, TR-05-20.

N.C.Y. Li (2011) Interactions of complex metal ion-humic and magnetite systems. PhD thesis, University of Manchester, p 67.

W. Li, H. Zhao, P. R. Teasdale, R. John & S. Zhang (2002) Application of a cellulose phosphate ion exchange membrane as a binding phase in the diffusive gradients in thin films technique for measurement of trace metals. Analytica Chimica Acta, 464, 331 – 339.

G. Lefevre, (2004). In situ Fourier-transform infrared spectroscopy studies of inorganic ions adsorption on metal oxides and hydroxides. *Advances in Colloid & Interface Science,* **107**(2), pp. 109.

W. Miller, R. Alexander, N. Chapman, I. McKinley, J. Smellie, 1994, Natural analogue studies in the geological disposal of radioactive waste. Studies in Environmental Science, 57.

T. Missana, Ú. Alonso, M. García-Gutiérrez, and M. Mingarro, 2008, Role of bentonite colloids on europium and plutonium migration in a granite fracture. Applied Geochemistry, 23, 1484-1497.

T. Missana, Ú. Alonso, M.J. Turrero, 2003, Generation and stability of bentonite colloids at the bentonite/granite interface of a deep geological radioactive waste repository. Journal of Contaminant Hydrology, 61, 17-31.

T. Missana, M. Garcia-Gutierrez and U. Alonso (2004). Kinetics and irreversibility of cesium and uranium sorption onto bentonite colloids in a deep granitic environment. *Applied Clay Science* **26**, 137-150.

T. Missana, M.Garcia-Gutierrez, U.Alonso, N.Albarran, M. Mingarro.Cesium migration in granite fractures in the presence of bentonite colloids: comparison between the Grimsel and the Äspö case. Abstract Accepted at the 2013 Migration Conference.

T. Missana, M. Garcia-Gutierrez and U. Alonso (2008b). Sorption of strontium onto illite/smectite mixed clays. *Physics and Chemistry of the Earth* **33**, S156-S162.
Missana, T., Alonso, U., Mayordomo, N., Garcia-Gutierrez, M. (2015) Cadmium adsorption onto Na-montmorillonite: experimental and modelling study. *CIEMAT publication (In press).*

T. Missana, M.Garcia-Gutierrez, U.Alonso, N.Albarran and M. Mingarro, 2013, Cs and bentonite transport experiments, in Understanding of Radionuclide Colloid Interaction (with special emphasis on sorption reversibility), pages 25 – 26, Deliverable 3.3 BELBaR Project Report, Eds. N.Bryan and N. Sherriff.

J. Monsallier, W. Schuessler, G. Buckau, T. Rabung, J. Kim, D. Jones, R. Keepax, N. Bryan, 2003, Kinetic Investigation of Eu(III)-Humate Interactions by Ion Exchange Resins. Analytical Chemistry, 75, 13, 3168-3174.

A. Möri, W.R. Alexander, H. Geckeis, W. Hauser, T. Schäfer, J. Eikenberg, T. Fierz, C. Degueldre, T. Missana, 2003, The colloid and radionuclide retardation experiment at the Grimsel Test Site: influence of bentonite colloids on radionuclide migration in a fractured rock. Colloids and Surfaces A: Physicochemical and Engineering Aspects, 217, 33-47.

J.D. Morton, J.D. Semrau, K.F. Hayes, 2001, An X-ray absorption spectroscopy study of the structure and reversibility of copper adsorbed to montmorillonite clay. Geochimica et Cosmochimica Acta, 65, 2709–2722.

K. Müller, H. Föerstendorf, V. Brendler and G. Bernhard (2009). Sorption of Np(V) onto TiO_2, SiO_2, and ZnO: an in situ ATR FT-IR spectroscopic study. *Environ Sci Technol,* **43**(20), pp. 7665.

K. Müller, H. Föerstendorf, T. Meusel, V. Brendler, M. J. Comarmond, G. Lefèvre and T. E. Payne (2012). Sorption of U(VI) at the TiO_2 – water interface: An in situ vibrational spectroscopic study. Geochimica et Cosmochimica Acta. 76, 191-205.

K. Müller, H. Föerstendorf, V. Brendler, A. Rossberg, K. Stolze, A. Ggöschel (2013). The surface reactions of U(VI) on γ-Al2O3 — In situ spectroscopic evaluation of the transition from sorption complexation to surface precipitation. *Chemical Geology,* **357**, pp. 75-84.

Nagra 1994, Technical Report, NTB 94-06.

M. Ochs, B. Lothenbach, M. Shibata, H. Sato, M. Yui, 2003, Sensitivity analysis of radionuclide migration in compacted bentonite: a mechanistic model approach. Journal of Contaminant Hydrology, 61, 313– 328.

P. M. Padilha, J. C. Rocha, J. C. Moreira, J. T. S. Campos & C. C. Federici (1997) Preconcentration of heavy metal ions from aqueous solutions by means of cellulose phospahate: an application in water analysis, Talanta, 45, 317 – 323.

D. L. Parkhurst & C. A. J. Appelo (1999) User's guide to PHREEQC (version 2) A computer program for speciation, batch-reaction, one-dimensional transport, and inverse geochemical calculations; U.S. Geological Survey: Denver, CO, USA, p 312

A. Pitois, P. I. Ivanov, L. G. Abrahamsen, N. D. Bryan, R. J. Taylor, H. E. Sims, 2008, Magnesium hydroxide bulk and colloid-associated 152Eu in an alkaline environment: Colloid characterization and sorption properties in the presence and absence of carbonate. Journal of Environmental Monitoring, 10, 315-24.

K. J. Powell, P. L. Brown, R. H. Byrne, T. Gajda, G. Hefter, A. K. Leuz, S. Sjöberg and H. Wanner (2011). Chemical speciation of environmentally significant metals with inorganic ligands. Part 4: The $Cd^{2+,}$ OH^{-}, Cl^{-}, $CO3^{2-}$, SO_4^{2-}, and PO_4^{3-} systems (IUPAC Technical Report). *Pure and Applied Chemistry* **83**, 1163–1214.

Th. Rabung, M.C. Pierret, A. Bauer, H. Geckeis, M.H. Bradbury and B. Baeyens, 2005, Sorption of Eu(III)/Cm(III) on Ca-montmorillonite and Na-illite. Part 1: Batch sorption and time-resolved laser fluorescence spectroscopy experiments. Geochimica et Cosmochimica Acta, 69, 5393–5402.

J.N. Ryan, M. Elimelech, 1996, Review: colloid mobilization and transport in groundwater. Colloid Surface A, 107, 1–56.

T. Schäfer, H. Geckeis, M. Bouby, T. Fanghänel, 2004, U, Th, Eu and colloid mobility in a granite fracture under near-natural flow conditions. Radiochimica Acta. 92, 731-737.

T. Schäfer, F. Huber, H. Seher, T. Missana, U. Alonso, M. Kumke, S. Eidner, F. Claret, F. Enzmann, 2012, Nanoparticles and their influence on radionuclide mobility in deep geological formations. Applied Geochemistry, 27, 390–403.

N. Sherriff, R. Issa and N.D. Bryan, 2013, Eu/Bentonite ternary systems, in Understanding of Radionuclide Colloid Interaction (with special emphasis on sorption reversibility), pages 14 – 23, Deliverable 3.3 BELBaR Project Report, Eds. N.Bryan and N. Sherriff.

N. Sherriff and N.D. Bryan, 2013, Colloid Kinetics in the Safety Case, in Understanding of Radionuclide Colloid Interaction (with special emphasis on sorption reversibility), pages 29 – 36, Deliverable 3.3 BELBaR Project Report, Eds. N.Bryan and N. Sherriff.

P. Steier et al. "The AMS isotope Uranium-236 at VERA" Presentation at the 13th International Conference on Accelerator Mass Spectrometry, 37, 24-29 August 2014, Aix en Provence, France.

P. Steier et al., (2010) "Analysis and application of heavy isotopes in the environment" Nucl. Instr. Meth. Phys. Res. Sect. B 268: 104-109.

W. Stumm (1992). "Chemistry of the solid-water interface. J. Wiley and Sons N.Y.
Zirino, A., and Yamamoto, S. (1972). A pH-dependent model for teh chemical speciation of copper, zinc, cadmium, and lead in seawater. *Limnology and Oceanography* **17**, 661-671.

T. Stumpf, C. Hennig, A. Bauer, M. A. Denecke, T. Fanghänel, 2004, An EXAFS and TRLFS study of the sorption of trivalent actinides onto smectite and kaolinite. Radiochimica Acta 92, 133–138.

S. Wold, 2010, Sorption of prioritized elements on montmorillonite colloids and their potential to transport radionuclides, SKB Technical Report, TR-10-20.